N° d'ordre : .....
N° de série : .....

People's Democratic Republic of Algeria
Ministry of Higher Education and Scientific Research

Final Year Project Report

Submitted at

The University of Echahid Hamma Lakhdar El Oued

Faculty of Technology
Department of Electrical Engineering
for fulfillment of the requirements for the Degree of

MASTER ACADEMIQUE

Réseaux électrique

By

Laid Hachef

And

Bousbia Laiche Souhaib

Theme

Real Time DC Motor Speed Control Based on LabVIEW Interfaced with Arduino

Defended on Jun 01, 2016. Before the jury:

Dr. Chemsa Ali	Associate Professor	President
Dr. Tir Zoheir	Associate Professor	Supervisor
Mr. Guemari Motazbillah	Substitute Professor	Co-supervisor
Dr. Bekakra Youcef	Associate Professor	Examinator

Academic Year 2015/2016

ACKNOWLEDGMENT

I would like to express my deepest thanks to all those people who influenced my work. I would like to add a few heartfelt words for the people who gave their unending support with warm wishes.

I would like to thank our supervisors, **Dr.Tir Zoheir** and **Mr.Guemari Motazbillah** for all the advices and guidance throughout my project. Without their continued support and interest, the project may be not as best as it is done.

I heartily acknowledge the cooperation and moral support of my family, and to my friends who always supported me in the entire course of study and thesis work.

Table of contents

List of Abbreviation and Symbols

SEDC : Self excitation Direct current

PID : Proportionnal Integral Derivation

VI : virtual instrument

GUI : graphical user interface

FTDI : Future Technology Devices International

LIFA :LabVIEW Interface for Arduino

ICSP : in-circuit serial programming

BDCM : Brushed Direct Current Motor

PWM : Pulse Width Modulation

List of Figures

ABSTRACT

The aim of this Final year project is to show how Separately Excited DC (SEDC) motor can be controlled by using a PID controller in LabVIEW. This control will be interfaced with LabVIEW using an Arduino board. The speed of the BDCM will be set by creating a Graphic User Interface (GUI) for PID Controller in LabVIEW.

The methodology during the project is divided into two parts which is software development and hardware implementation. The works in software development are calculation of SEDC motor transfer function, simulation to determine the parameter value of PID and developing the software controller. Ziegler-Nichols Closed-Loop Method is used to obtain the value for K_p and K_i. The last part is to interface the controller with the hardware.

Chapter I

Introduction

1. Background

SEDC motor have been widely use in high-performance electrical drives and servo system [1]. There are various differences SEDC motors in the market and all with it good and bad attributes. Such bad attribute is the lag of efficiency. In order to overcome this problem a Proportional–Integral–Derivative (PID) controller is introduce to the system. PID controller is a generic control loop feedback mechanism widely used in industrial control systems [1]. A PID controller attempts to correct the error between a measured system variable and a desired set point by calculating and then outputting a corrective action that can adjust the systeme accordingly. So, by integrating the PID controller to the SEDC motor were able to correct the error made by the BDC motor and control the speed of the SEDC motor to the desired speed.

2. Objective

The objectives of this project are:

i. To explorer and apply the knowledge gain in lectures into practical applications.
ii. to derive mathematical model of SEDC motor and develop PID controller for the motor,
iii. To control the speed of SEDC motor with PID controller interfaced with LabVIEW using an Arduino board.
iv. Analysis the experimental result using the actual motor.

3. Scope of Work

The scope of this project is;

i. Design, modeling and simulation of the PID controller with the SEDC motor
ii. Implementation of the PID controller with and actual SEDC motor
iii. The experimental results with the actual SEDC motor

4. Problem Statement

The problem encounter when dealing with SEDC motor is the lag of efficiency and losses. In order to eliminate this problem, PID controller is introduced for the SEDC motor. This is because PID controller helps get the output, where we want it in a short time, with minimal overshoot and little error.

5. Thesis Organization

This thesis is organized with the Overview of DC motors, including the equations that represent torque, rotor speed, field and armature currents and voltages, covered in Chapter II.

Design and Modeling of Buck Converter for drive system are detailed in Chapter III. Test setup and results for each test is presented and performance is explained in detail.

Identification and PID Controller of a 1st Order DC Motor Model is discussed in Chapter IV.

Results of the testing and conclusions about the Speed Control of DC Motor performance are addressed in Chapter V. Recommendations on future work are suggested for additional research regarding DC motor controlled.

Date sheets for equipment used, LabView code, Graphical User Interface (GUI) are detailed in the Appendixes.

Chapter II

DC Motor Overview

1. Introduction to DC Motors

To understand how to control output speed of a DC motor, a review some of the basics of DC motor operations and theire types and construction was introduced in this section.

The DC motor is a machine which converts electrical energy into mechanical energy. It uses magnetism produced by electric current flowing in the armature windings, to produce mechanical rotation. One side is a field circuit that is used to produce a field flux and the other side is an armature circuit that provides current to the rotor via brush and commutator. The interaction of the field flux and armature current in the rotor produces speed. [4].

2. Construction

A DC motor consists of two main parts:

í) **Stationary part:** it is designed mainly for producing a magnetic flux.

íí) **Rotating part**: it is called the armature, where electrical energy is converted into mechanical energy.

The stationary and the rotating parts are separated from each other by an air gap.

- The stationary part of a D.C motor consists of main poles, designed to create the magnetic flux, commutating poles and designed to ensure sparkles operation of the brushes at the commutator (in very small machines with a lack of space commutating poles are not used), and a frame /yoke.
- The armature is a cylindrical body rotating in the space between the poles and comprising a slotted armature core, a winding inserted in the armature core slots, a commutator, and brushes.

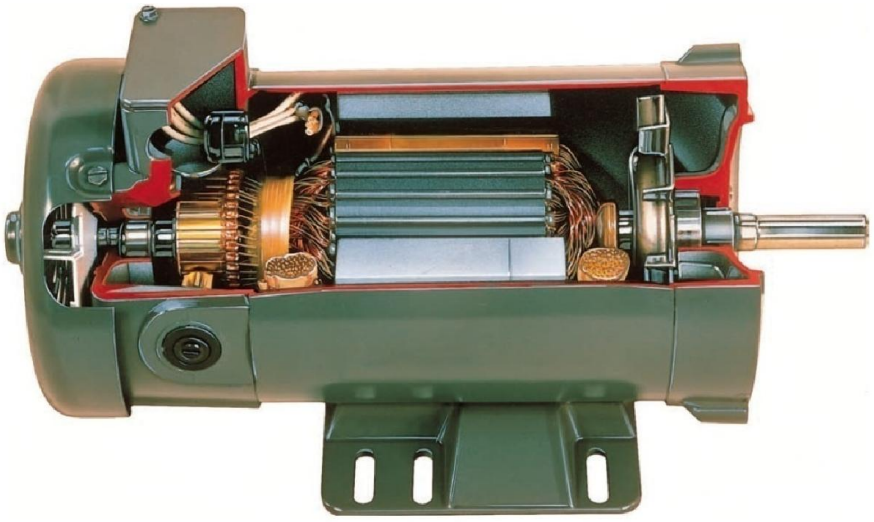

Figure 1 DC motor constraction [15]

3. Principle of operation

A DC motor consists of a stator poles and a wound rotor. Connection to the rotor windings is made with brushes, which make contact with a commutator that is affixed to but insulated from the shaft. When power is applied, the rotor rotates to align its magnetic field with the stator. Just as the field is aligned, the commutator sections that had been in contact with the brushes brake contact and the adjacent commutator sections make contact this causes the polarity of the windings to reverse. The rotor then tries to align its new magnetic field with the stator. The rotor rotates because the brushes keep changing the winding polarity.

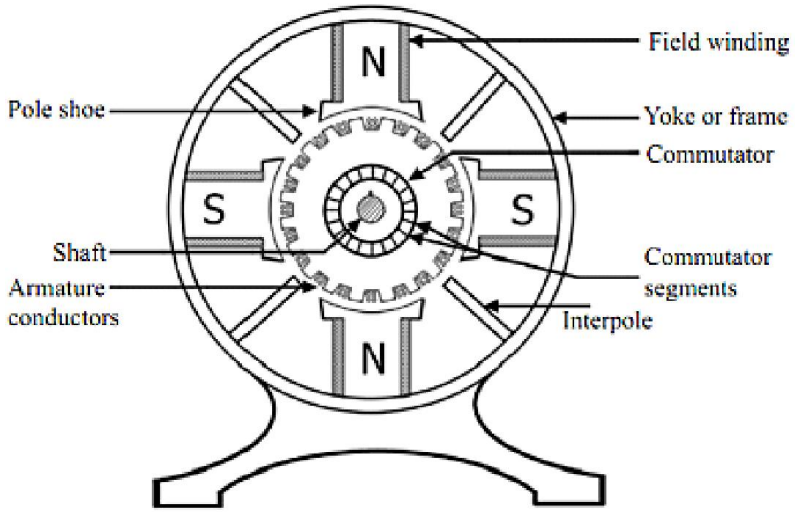

Figure 2 Cross-section of DC motor [16]

4. Classification of D.C motors

Direct current motors are classified into three types, drawing their name from the way in which their field windings are electrically connected to the armature. Each type has its own specific load-speed characteristics, as well as certain preferred applications. The three categories are the shunt, series, and compound DC motors, as shown in Figure 3.

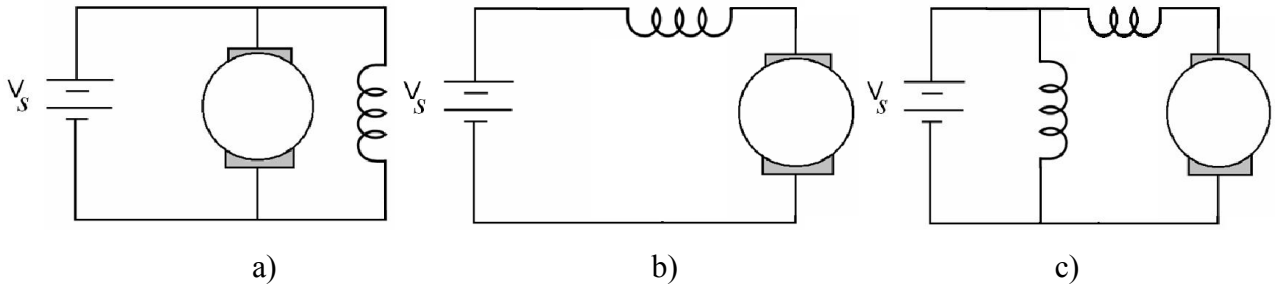

Figure 3 types of DC motor : a) Shunt field b) Series field c) Compound

5. Separately excited DC motor

Figure.4 shows the equivalent circuit for a separately excited DC motor. When a separately excited DC motor is exited by a field current of i_f and an armature current of i_a flows in the armature winding, the motor develops a back emf and a torque to balance the load torque at a particular speed. The field current of a separately excited motor is independent of the armature current and any change in the armature current has no effect on the field current. The field current is normally much less than the armature current.

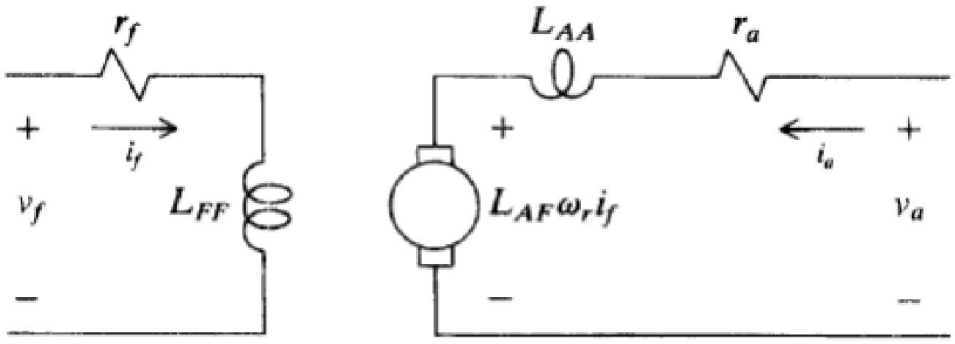

Figure 4 Equivalent circuit of a SEDC machine. [4].

The field voltage and armature voltage are defined in matrix form as:

$$\begin{bmatrix} v_f \\ v_a \end{bmatrix} = \begin{bmatrix} r_f + s\,L_f & 0 \\ \omega_r\,L_{af} & r_a + s\,L_{aa} \end{bmatrix} \begin{bmatrix} i_f \\ i_a \end{bmatrix} \qquad (2.1)$$

where i_f and i_a are the field and armature currents, r_a and r_f are the armature and field resistance, and L_{aa} and L_{aa} are the self-inductance of the armature and field windings, respectively. L_{af} is the mutual inductance between the armature and field windings, and ω_r is the rotor speed.

An equivalent circuit of a SEDC machine, shown in Figure 2, defines where these variables are identified. On the right side of Figure 2, or the armature circuit side, the voltage induced from the motor action is equal to $L_{af}\,\omega_r\,i_f$. This is sometimes referred to as the back emf. $L_{af}\,\omega_r\,i_f$ also represents the open-circuit armature voltage v_a [4].

Electric torque T_e is defined by its mutual inductance and the field and armature current as

$$T_e = L_{af}\,i_f i_a = \lambda_f i_a \qquad (2.2)$$

Electric torque is equivalent to mechanical torque and is defined as

$$T_e - T_L = J\,s\,\omega_r + B_m\,\omega_r \qquad (2.3)$$

where J is the inertia of the rotor, B_m is the damping coefficient, T_L is the load torque that opposes the electric torque.

1. Steady-state torque and speed 4

Separate excitation is a basic DC motor setup that is similar to Figure 3 with the exception of a variable field rheostat is added to it. A field rheostat is used to adjust the field current in the circuit.

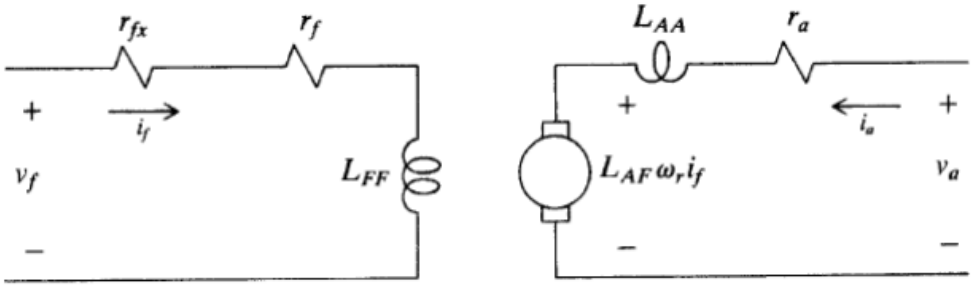

Figure 5 Equivalent circuit for separate field and armature excitation [4]

The field voltage when the SEDC motor is at steady state is defined as

$$v_f = r_f\, i_f \qquad (2.4)$$

The total field resistance r_f is equal to the field rheostat value r_{fx} plus the field circuit resistance r_f. The capital letter denotes steady state values for current and voltage [4].

The armature voltage at steady-state operation is

$$v_a = r_a\, i_a + \omega_r L_{af} i_f \qquad (2.5)$$

Rearranging Equation (2.5) to solve for i_a, we get

$$i_a = \frac{v_a - \omega_r L_{af} i_f}{r_a} \qquad (2.6)$$

Substituting Equation (2.6) into (2.2), we get

$$T_e = L_{af} i_f \left(\frac{v_a - \omega_r L_{af} i_f}{r_a}\right) \qquad (2.7)$$

The mutual inductance L_{af} has a constant value. If the field voltage v_f and total field resistance r_f are held to a constant value, i_f will stay constant.

From Equation 2.7, we can now predict the electric torque T_e at a given speed ω_r if the armature voltage v_a is constant at steady-state conditions. Inversely, we can also predict ω_r at a given T_e for a constant v_a.[4]

In practice, for a speed less than the base speed , the armature current and the field current are maintained constant to meet the torque demand, and the armature voltage, is varied to control the speed. For speed higher than the base speed, the armature voltage is maintained at the rated value and the field current is varied to control the speed .the power developed by the motor remains constant. Fig.2.5 show the characteristics of torque, power, armature current ,and the field current against the speed .

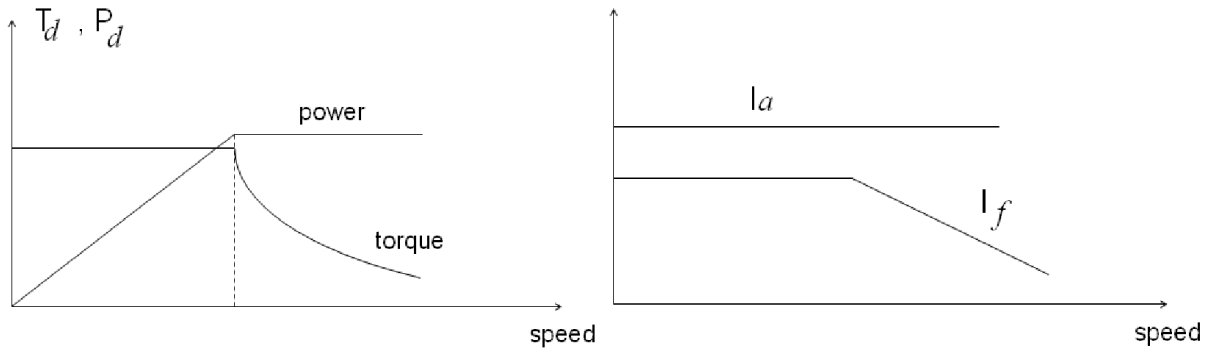

Figure 6 (a, b) Typical characteristics of a separately excited D.C motor.

6. Speed regulation

A motor which is able to maintain its speed at constant level when a variable load is applied to it, it has good speed regulation. It is a built in characteristic of a motor and remains the same as long as the applied voltage kept constant. Speed regulation of a motor is a comparison of it's no load speed to its full-load speed and is usually expressed in a percent as follows:

$$\text{Percent speed regulation} = \frac{(noload - speed) - (fullload - speed)}{fullload - speed} \times 100\ \%$$

The lower of the speed-regulation percent of a motor, the better is the speed regulation. If the speed –regulation percent is high, then its speed regulation is poor.

7. Motor losses

The losses of a D.C motor may be divided into two types mechanical and copper losses.

a) Copper losses (I^2R), are present in the armature windings, the shunt field, the series field, and the interpole field windings . The I^2R losses depend on the effective resistance
of these windings. Power is used whenever a current flows through these resistances. these resistances maybe found by the ammeter – voltmeter method ; they are then multiplied by the currents squared to obtain the copper losses .

b) Mechanical or rotational losses are divided into two groups: the iron (or core losses), and friction losses. Iron losses consist of the eddy current loss and hysteresis losses.

8. Applications

Because of their inherent characteristics direct current motors are used in application where exacting control characteristics are very important such as cranes, elevators, numerical control, tape drives, and data processing. They are also used in the field of transportation, in vehicles such as electric buses and streetcars.

9. Advantages

The D.C motors have the following advantages:

- High starting torque.
- Speed control over a wide range, both below and above the normal speed.
- Quick starting, stopping, reversing and accelerating.

10. Disadvantages

The disadvantages of DC motors are:

- High initial cost.
- Increased operating and maintenance costs because of the commutators and brushes.

11. Equipment Setup for Performance Testing of Theory

Some of the components used in this experiment. The equipment used for this experiment and shown in Figure 7 and detailed: Converter Buck based IGBT, AC/DC Power Supply, 180W DC motor, Electrodynamometer, Tachometer, Computer with Labview Software, Oscilloscope and Multimeters.

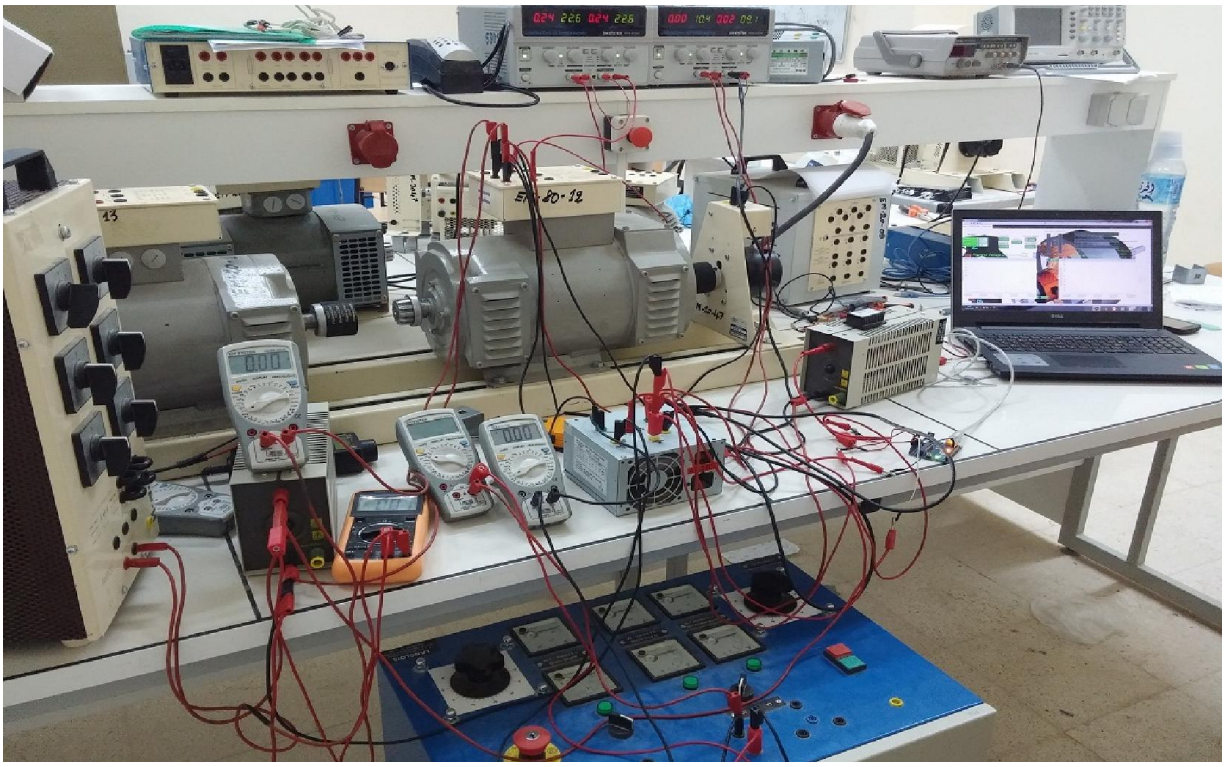

Figure 7 Photograph of equipment used.

In Figure 4, a schematic diagram of the equipment setup for this experiment is shown.

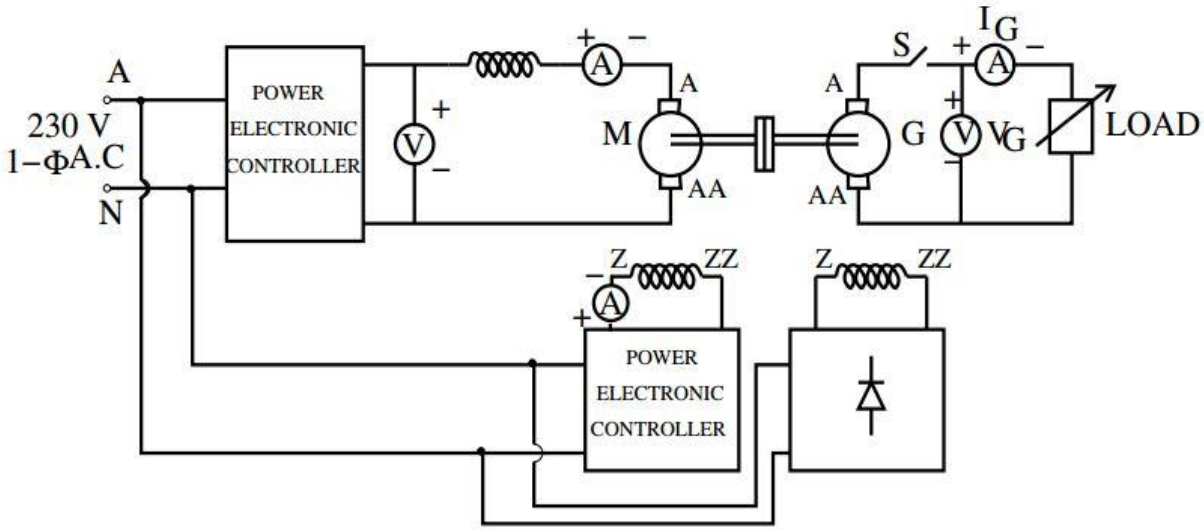

Figure 8 Circuit diagram for speed control of SEDC motor

Chapter III

Design and Modeling of Buck Converter

1. Modeling of (Chooper) Buck Converter

Buck converter (BC) is very interested for improve the performance and controllability of industrial applications such as speed control of DC motors, subway cars, trolley buses and battery operated vehicles etc.[9]

Buck converter is a basically static power electronics device which converts fixed dc voltage / power to variable DC voltage or power. It is nothing but a high speed switch which connects and disconnects the load from source at a high rate to get variable or chopped voltage at the output [9]. It produces a lower average output voltage than the SEDC input voltage V_s. Its main application is in regulated DC power supplies and SEDC motor speed control [8].

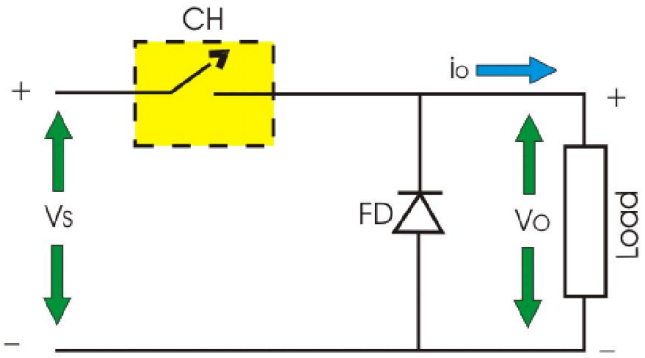

Figure 9 Simplifed Buck Converter Circuit Diagram [5]

The Practical design of buck converter is used in this project for speed control of SEDC motor is shonw as in Figure 7

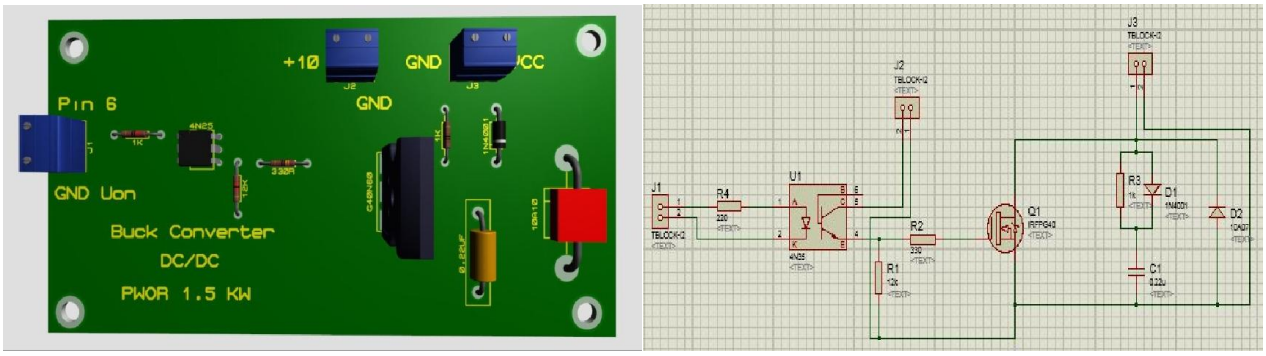

Figure 10 Practical design of buck converter for DC motor.

Conceptually, the basic circuit of Fig. 6 constitutes a buck converter for a load (R or RL or RLE).

A transistor type used in buck converter is **Ultra-Fast IGBT**. This device is represented as a switch in a dotted box for simplicity. When it is closed current can flow in the direction of arrow only.

Figure 11 Ultra-Fast IGBT [see Appendex]

A. Operation of Buck converter with Resistive Load

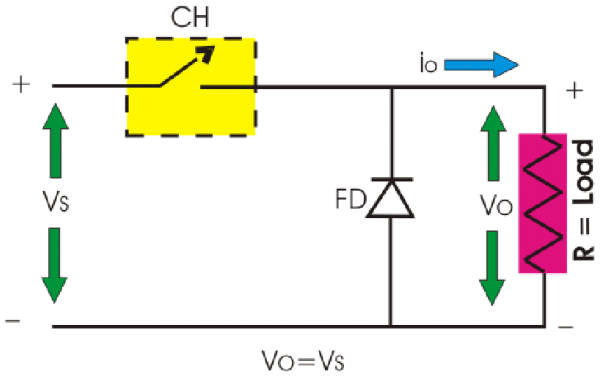

Figure 12 Operation of Buck Converter with Resistive Load [9]

When CH is ON, $V_O = V_S$, when CH is OFF, $V_O = 0$

Average output voltage is calculated by:

$$V_o = \frac{1}{T_s}\int_o^{T_{ON}} V_s(t)\,dt = \frac{V_s T_{on}}{T} = DV_s \qquad (3.1)$$

Where,

D = Ton/T is duty cycle and $(0 \leq D \leq 1)$

T_{ON} can be varied from 0 to T, so $0 \leq D \leq 1$. Hence output voltage V_O can be varied from 0 to V_S.

RMS output voltage is calculated by:

$$V_{or} = \sqrt{\frac{1}{T}\int_o^{T_{ON}} V_s^2(t)\,dt} = V_s\sqrt{\frac{T_{on}}{T}} = V_s\sqrt{D} \qquad (3.2)$$

The practical instantaneous output voltage and current waveform of buck converter with Resistive Load equal to 100 Ohm is shown below (Figure 10).

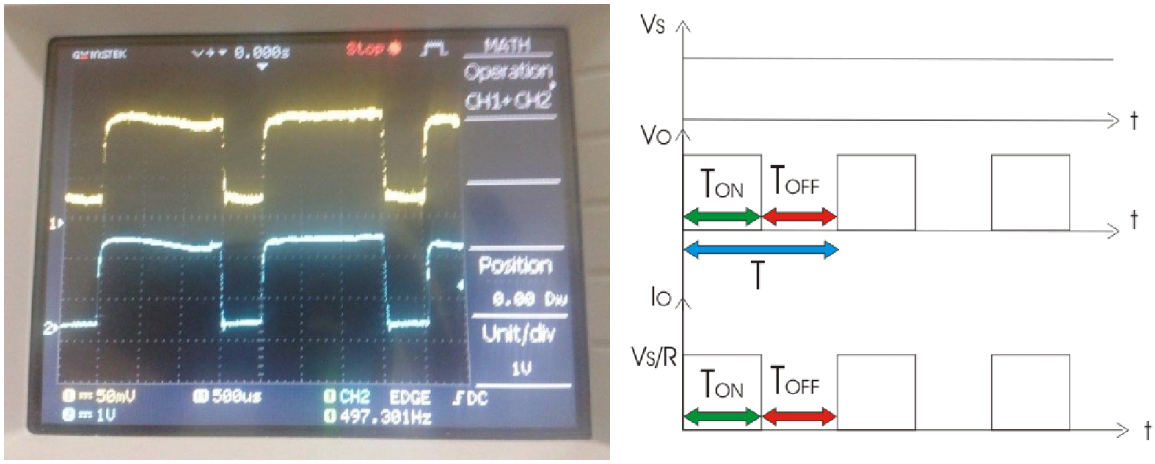

Figure 13 Practical instantaneous output voltage and current of BC with resistive load.

where

T_{ON} : It is the interval in which chopper is in ON state.

T_{OFF} : It is the interval in which chopper is in OFF state.

V_S : Source or input voltage.

V_O : Output or load voltage.

T : Chopping period = $T_{ON} + T_{OFF}$.

B. Operation of Buck Converter with Inductive Load

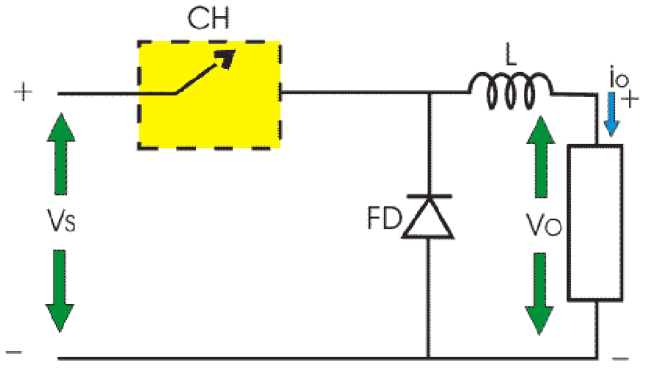

Figure 14 Operation of Buck Converter with Inductive Load [9]

During ON time of converter

$$V_s = V_L + V_o \implies V_L = V_s - V_o \implies L\frac{di}{dt} = L\frac{\Delta i}{T_{ON}} = V_s - V_o \qquad (3.3)$$

Therefore, peak to peak load current,

$$\Delta i = \frac{V_s - V_o}{L} T_{ON} \qquad (3.4)$$

During OFF Time of Chopper

When CH is OFF inductor reverses its polarity and discharges.

This current freewheels through diode FD.

$$L\frac{di}{dt} = V_o$$

$$L\frac{\Delta i}{T_{OFF}} = V_o \Rightarrow \Delta i = V_o\frac{T_{OFF}}{L} \qquad (3.5)$$

By equating (3.4) and (3.5)

$$\frac{V_s - V_o}{L}T_{ON} = \frac{V_o}{L}T_{OFF} \Rightarrow \frac{V_s - V_o}{V_o} = \frac{T_{OFF}}{T_{ON}} \Rightarrow \frac{V_s}{V_o} = \frac{T_{ON} - T_{OFF}}{T_{ON}}$$

There fore,

$$V_o = \frac{T_{ON}}{T}V_s = DV_s \qquad (3.6)$$

So, from (3.4) we get,

$$\Delta i = \frac{V_s - DV_s}{L}\,DT\left[Since, D\frac{T_{ON}}{T}\right] = \frac{V_s(1-D)D}{Lf}\left[f = \frac{1}{T} = Chopping\ Frequency\right] \quad (3.7)$$

The Chopping frequency is 1 KHz, and the input voltage is 140V.

The practical instantaneous output voltage and current waveform of buck converter operation with inductive Load (L=0.7 H and R=5.4 Ω) is shown in below (Figure 11)

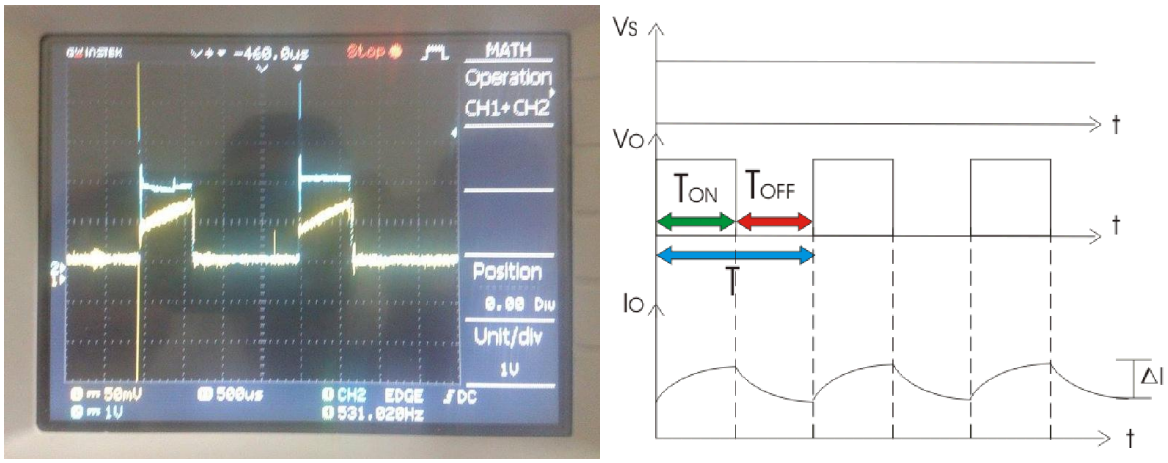

Figure 15 Practical instantaneous output voltage and current of BC with inductive load

2. Control Strategie of Buck Converter

The average value of output voltage V_o can be controlled through Duty Cycle by opening and closing the semiconductor switch periodically.

The control strategie for varying duty cycle in this project is an Arduino UNO using Pulse Width Modulation (PWM) technique. PWM is a technique for supplying electrical power to a load that has a relatively slow response. The supply signal consists of a train of voltages pulses such that the

width of individual pulses controls the effective voltage level to the load. The PWM pulse train acts like a DC signal when devices that receive the signal have an electromechanical response time that is slower than the frequency of the pulses. For a DC motor, the energy storage in the motor windings effectively smooth's out the energy bursts delivered by the input pulses so that the motor experiences a lesser or greater electrical power input depending on the widths of the pulses. The formula below shows the voltage signal comprised of pulses of duration T_{ON} that repeat every T_{OFF} units of time. The output of a PWM channel is either Vs volt during the pulse or zero volts otherwise. If this signal is supplied as input to a device that has a response time much larger than T_{OFF}.[11]

The effective DC voltage supplied to the load is controlled by adjusting the duty cycle. On an Arduino Uno, PWM output is possible on digital I/O pins 3, 5, 6, 9, 10 and 11. On these pins the analogWrite function is used to set the duty cycle of a PWM pulse train that operates at approximately 1000 Hz. Thus, with a frequency fc = 1000 Hz, the period is T_{OFF} = 1/fc ~2ms. The PWM output level with the analogWrite is an 8-bit value that corresponds to an effective voltage range of 0 to 5 V, [11]. The relationships between the effective DC voltage supplied and PWM output parameters as in below:

$$PWM = 255\ \frac{T_{ON}}{T_{OFF}} = \ 255\ \frac{V_{Or}}{V_s} \qquad (3.8)$$

Chapter IV

Identification and PID Controller of a 1st Order DC Motor Model

1. Objective

The response of a first order DC Motor depends on its DC gain, *K*, and time constant, τ. Both K and τ are function of DC Motor parameters. The objective of this chapter is to model a first-order DC Motor and investigate the effect of DC Motor parameters on its response to a step input.

We choose to experiment with an armature controlled DC motor, which behaves as a first-order machine when the armature voltage is the input and the angular speed is the output. We obtain the transfer function of the DC motor and identify specific parameters of the system that affect system response. Specifically, we identify system parameters that individually affect the DC gain and the time constant and vary these parameters to experimentally verify the change in system response, [12].

2. Background

2.1. First-order systems

The standard form of transfer function of a first-order system is:

$$G(s) = \frac{Y(s)}{U(s)} = \frac{K}{(\tau s + 1)} \tag{4.1}$$

where $Y(s)$ and $U(s)$ are the Laplace transforms of the output and input variables, respectively, K is the DC gain, and τ is the time constant. For a unit step input $U(s) = 1/s$, the response of the system is:

$$Y(s) = \frac{Y(s)}{U(s)} U(s) = \frac{K}{(\tau s + 1)} \frac{1}{s} = \frac{K}{s(\tau s + 1)} \tag{4.2}$$

The inverse of the resulting Laplace transform can be easily found (see the Appendix in your text). Typically the inverse is available in standard tables. In this case,

$$y(t) = L^{-1}\left[\frac{K}{s(\tau s + 1)}\right] = K\left\{L^{-1}\left[\frac{1}{s(\tau s + 1)}\right]\right\} = K(1 - e^{-t/\tau}) \tag{4.3}$$

It is clear from (3)) that $y \to K$ as $t \to \infty$. The DC gain can therefore be interpreted as the final value of the output for a unit step input. The time constant is the time required for $y(t)$ to reach 63.2% of its final value. Indeed, at $t = \tau$, $y(t) = 0.632K$ for a unit step input. For a unit step input, the change in input is one (1). In general, for a step input of magnitude A, at $t = \tau$, $y(t) = 0.632KA$. The response of the first-order system to a unit step input is shown in Fig.1a for two cases. For a system gain $K < 1$, the system's output change is less than the input change applied. For a system gain $K > 1$. the system's output change is more than the input change applied. The results plotted are for a system operating for small positive input and output deviations from zero (the origin) [12].

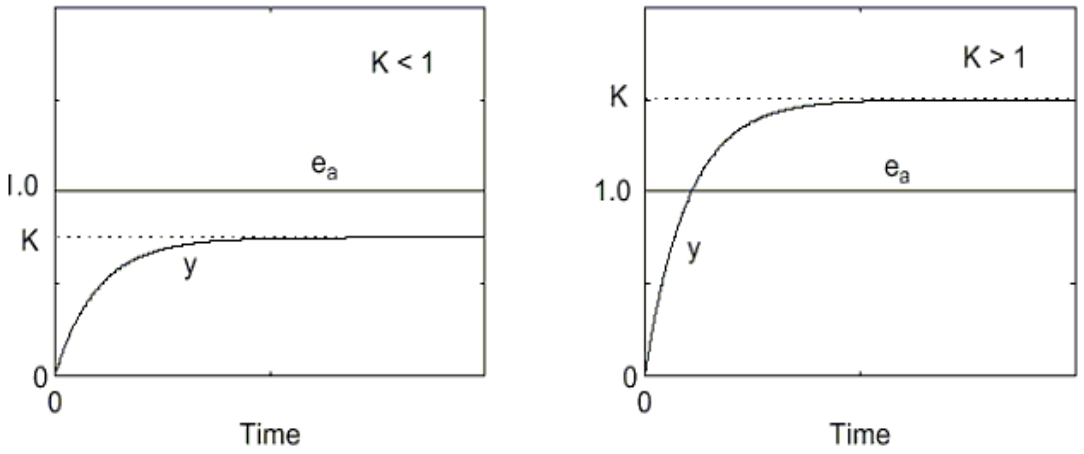

Figure 16: First-Order System Step Response

The step response of the DC motor will be evaluated with a square wave input composed of a series of positive and negative steps. As shown in Figure 16, these steps produce repeated positive and negative changes in a 1st order system's output. Assuming the positive system's response reaches steady-state for each positive and negative input, the gain and time constant parameters can be separately evaluated for both positive and negative input changes. The specific values for the gain and time constant parameters for the above systems are computed below. Notice that the system gains are equal but that the positive and negative change time constants are not. For both parameters, an average is typically used as a representative value. The variation from the average indicates the repeatability of the measurement, [12].

2.2 DC Servo Motor System

An experimental schematic diagram of an armature controlled DC motor is shown in Figure 17. The system variables include:

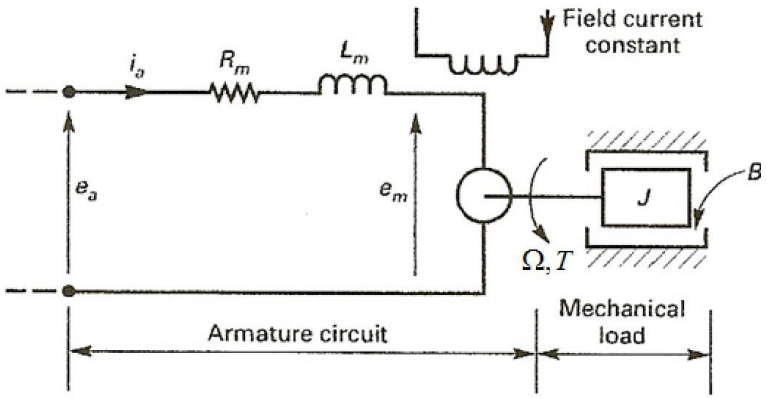

Figure 17: The DC motor (Phillips and Harbor) [12]

e_a : Armature drive potential (volts).

e_m : Back emf potential (volts)

i_a : armature current (Amps)

T : torque produced by motor (N-m)

θ : angular position of motor shaft (radians)

$\Omega = d\theta/dt$: angular velocity of motor shaft (rad/sec)

The parameters of the system include:

R_m : Armature resistance (Ohms)

L_m : armature inductance (Henry)

J : moment of inertia of motor shaft (Kg-m^2)

B : coefficient of viscous friction (N-m-sec/rad)

The system parameters not shown in Fig.2 include:

K_T : Torque constant (N-m/Amp)

K_b : motor back emf constant (volt-sec/rad)

The torque constant K_T models the relationship between the electric current i_a input and motor torque T output.

$$T(s) = K_T i_a(s) \tag{4.4}$$

The back EMF constant K_b models the relationship between the motor speed Ω input and the electrical back emf e_b produced by the DC motor,

$$e_m(s) = K_b \Omega(s) \tag{4.5}$$

The transfer function of the servomotor, with armature drive potential e_a as input and motor speed $\Omega = s\theta(s)$ as output, can be written as (Phillips and Harbor, Section 2.72)

$$G(s) = \frac{\Omega(s)}{e_a(s)} = \frac{K_T}{JL_m s^2 + (BL_m + JRm)s + (BR_m + K_T K_b)} \tag{4.6}$$

Typically, the inductance of the motor armature is relatively small. Neglecting the armature inertia L_m, yields the low speed approximation for the DC servo motor transfer function

$$G(s) = \frac{\Omega(s)}{e_a(s)} = \frac{K_T}{JR_a s + (bR_a + K_T K_b)} \tag{4.7}$$

Rewriting (4.7) is the standard 1st order transfer function form (1) yields

$$G(s) = \frac{\omega(s)}{e_a(s)} = \frac{K_T/(bR_a + K_T K_b)}{[JR_a/(bR_a + K_T K_b)]s + 1} \tag{4.8}$$

and comparing it with (1), we obtain the expression for the motor DC gain:

$$K_m = \frac{K_T}{(bR_a + K_T K_b)} \tag{4.9}$$

and the DC motor time constant:

$$\tau_m = \frac{JR_a}{(bR_a + K_T K_b)} \tag{4.10}$$

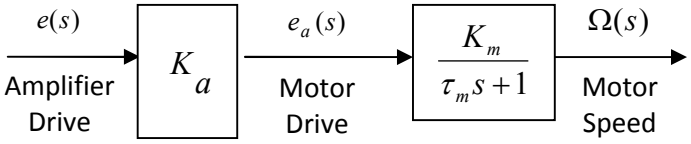

Figure 18: Block Diagram of the Motor and Amplifier System.[12]

An amplifier is often used to generate the power required to drive the armature voltage on the motor. A block diagram showing an amplifier connected to the motor transfer function is shown in Fig. 18. The amplifier modeled as a constant gain K_a, is also shown.. Together, the motor and the amplifier can be modeled as a single first-order system with steady-state (DC) gain:

$$K = \frac{K_a K_T}{(bR_a + K_T K_b)} \tag{4.11}$$

and the time constant:

$$\tau = \frac{JR_a}{(bR_a + K_T K_b)} \tag{4.12}$$

Comparing (4.9) and (4.11), the DC gain K of the motor and amplifier system is the product of the motor DC gain K_m and the gain of the amplifier K_a.

$$K = K_a * K_m \tag{4.13}$$

A comparison of (4.10) and (4.12) indicates that the time constant τ of the motor plus amplifier system is the same as the motor time constant τ_m alone. One of the primary objectives of this experiment is to study those effects that vary the system's DC gain and the time constant. Although it is possible to vary the system's DC gain K by varying the amplifier gain K_a, we will not vary K_a in this experiment. We will vary the system's time constant τ by changing the inertia of the motor shaft *J* by mounting an inertia disk on the motor shaft. The above analysis shows that we expect these two changes to have independent effects on the motor system response.

2.3 Experimental Procedure:

The overall experimental setup is shown schematically in Figure 8

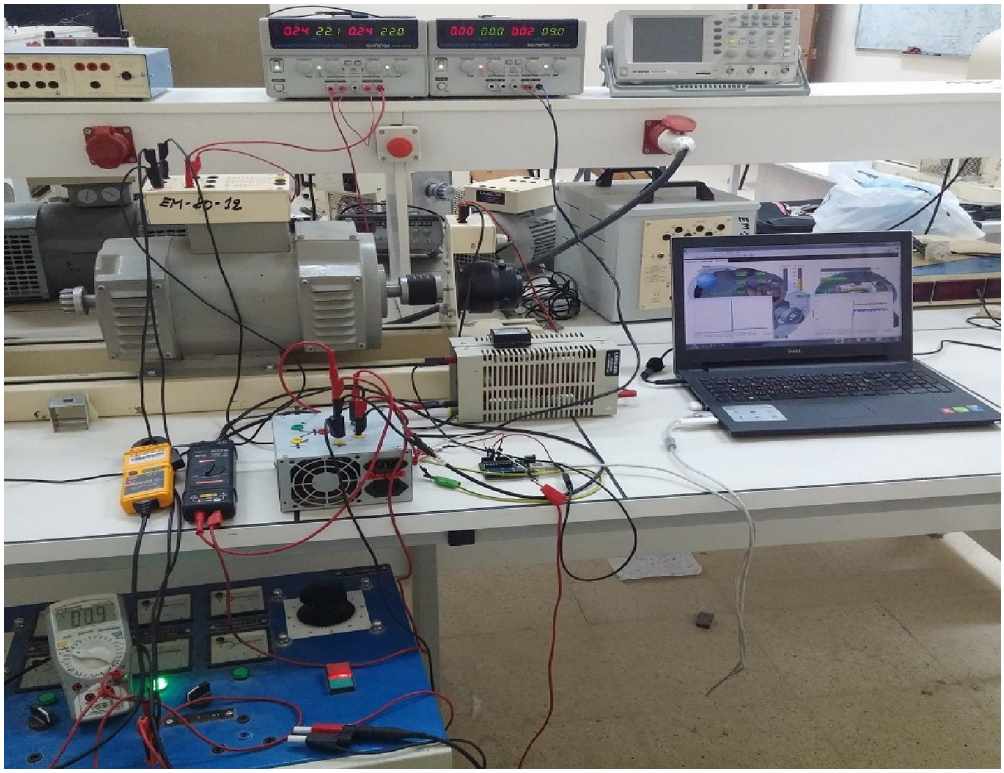

Figure 19 Basic Equipment Setup

According the experimental result below, the gain of the DC Motor is = 117.5 rd/s, the time constant of the DC Motor is = 0.15 s

Figure 20 Step response methode.

The first-order system below is composed of an amplifier and a plant. Find the system transfer function in standard first-order form, K/(τs+1).

3. Experimental Tuning of PID Controllers via Ziegler-Nichols Methods

Until 1941, the engineers, John Ziegler and Nathaniel Nichols have changed the whole control industry by theire tuning methode. John Ziegler was the practical one of the pair with a lot of experience in process applications, and who performed all the simulator tests that led to the

methods they were seeking. Nathaniel Nichols was the mathematician and who reduced all of the mathematics to a few simple relationships that could be understood by technicians and operators. The results were the now famous "Ziegler-Nichols" methods of tuning controllers - methods that survived the slings and arrows of its early detractors, withstood the test of time, and works just as well as many of the later more sophisticated optimizing forms on a great majority of process applications.[13]

3.1 The step response method

The Ziegler-Nichols step response method is based on a step response of the DC motor. A step input is made in the control signal to the DC Motor and the response is logged for analysis Figure 20.

The DC Motor characteristics which have determined from the DC Motor in the following way:[13]

i. Locate the point on the DC Motor response curve where the slope is greatest, and draw the tangent to the curve through this point.

ii. Find the points at which this tangent cuts the two lines which give the stationary values of the DC motor variable before and after the step disturbance respectively.

iii. Reading off the times for these two points, the dead-time (L=10 ms, see fig.20) and the dominant time constant (T=150 ms, see fig.20) for the DC Motor. The dead-time is defined as that time it took from when the step disturbance was made until the DC Motor signal began to react. With the Ziegler-Nichols method for determining dead-time, the estimated dead-time is often longer than it is in real life. This is correct, and it is due to the very simple model of the DC Motor which is used since high-order dynamics also appear in the step response as an additional dead-time. In other words, the dead-time L and the time constant T have to describe a DC Motor which may comprise one dead-time and several time constants. This is approximated with a slightly longer dead-time and a dominant time constant.

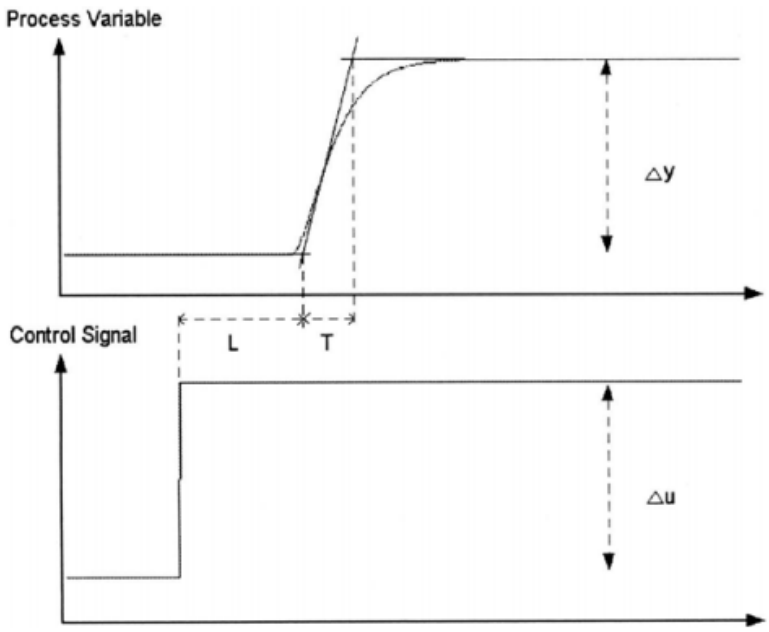

Figure 21 Step response method

iv. The static gain Kp of the DC Motor is estimated by taking the ratio between the process variable change and the control signal change:

$$K_p = \frac{\Delta\omega}{\Delta \mathrm{u}} = \frac{117.5\, rd/s}{100\, V} = 1.175\, rd/sV.$$

Based on these three parameters L, T and K_p determined from the step experiment (see figure 20), the Ziegler-Nichols step response method can now provides the controller parameters such as in table 1. In order to simplify the table, the relationship between the dead-time and the time constant has been designated by θ, where

$$\theta = \frac{L}{T} = 0.067$$

The constant θ is known as the normalized dead-time. The Ziegler-Nichols table was originally drawn up for the PID controller in its parallel design type.

Tableau 1 PID parameters according to Ziegler-Nichols step response method.

Controller	K	T_i	T_d
P	$\frac{1}{K_p\theta} = 12.7$	-	-
PI	$\frac{0.9}{K_p\theta} = 11.43$	3L=0.03	-
PID	$\frac{0.6}{K_p\theta} = 7.62$	2L=0.02	L/2=0.01

In the table, the controller gain is inversely proportional to the static gain of the DC motor and the normalized dead-time.

Both the integral and derivative times are proportional to the dead-time of the DC motor. This is also sensible, because the time parameters of the controller have to lie in the same range as the DC motor time scale.

3.2 Advantage of the Ziegler-Nichols

The main advantage of the Ziegler-Nichols step response method is in its simplicity as only a step experiment is required. The disadvantage is that the method is relatively sensitive to load disturbances and other disturbances in the frequency range of interest during the experimental phase and a large step input may be necessary to obtain a good signal-to-noise ratio. On the other hand, use of a large input is restricted by the non-linear modes of the DC motor as well as important safety operational limits [13].

Chapter IV

Speed Control of DC Motor

1. Overview

Here in this chapter terminal voltage control method is employed. A control system is an interconnection of components forming a system configuration that will provide a desired system response. A controlled DC motor is developed allowing Arduino hardware which acts as the interface between the computer LabVIEW and the outside world. It primarily functions as a device that digitizes incoming analog signals so that the LabVIEW can interpret them. The user interface was developed in an Arduino environment. The aim is to control the speed of the dc motor using the Low Cost data acquisition board i.e. the Arduino board interfaced with PID Controller in LabVIEW.[11]

2. Arduino Uno Board

The Arduino Uno is a microcontroller board based on the ATmega328. It has 14 digital input/output pins (of which 6 can be used as PWM outputs), 6 analog inputs, a 16 MHz ceramic resonator, a USB connection, a power jack, an ICSP header, and a reset button. It contains everything needed to support the microcontroller; simply connect it to a computer with a USB cable or power it with an AC-to-DC adapter or battery to get started.[11]

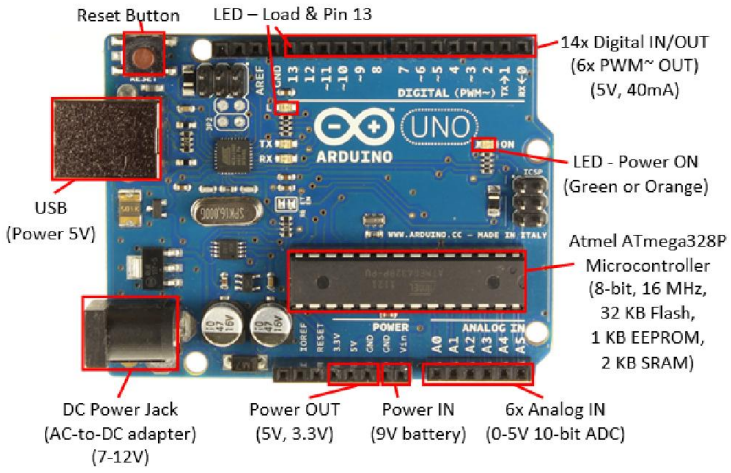

Figure 22: Arduino Uno Front and Back

The Uno differs from all preceding boards in that it does not use the FTDI USB-to-serial driver chip. Instead, it features the Atmega16U2 (Atmega8U2 up to version R2) programmed as a USB-to-serial converter.

A sketch for the Arduino microcontroller acts as an I/O engine that interfaces with the LabVIEW Vis through a serial connection. This helps to move information from Arduino to LabVIEW without adjusting the communication, synchronization or even a single line of code. Using the Open, Read/Write, Close convention in LabVIEW we can access the digital, analog and pulse width

modulated signals of the Arduino microcontroller. The Arduino microcontroller must be connected to the computer with the LabVIEW through a USB…[11]

3. LabVIEW Interface for Arduino LIFA

Labview is the main software used. Labview interfacing with arduino allows users to get data from Arduino microcontroller and the data processed by Labview Graphical Programming environment. Labview is Laboratory Virtual Instrumentation Engineering Workbench which is a graphical programming language. It was released in 1986 by National Instruments, [14]

LIFA is the main part for this system as the data and control system will do by it. Labview is chosen as the software for this system because it is easy to implement as it is graphical programming. Furthermore, Labview supports in GUI building, Labview use dataflow paradigm and automatic memory management. The interest on visual programming makes the Labview as the chosen software. GUI based system allow users to set monitoring parameter, to read value from sensor, to acquire data and to display important parameter. Other than that, Labview is suitable for An Automatic Fertigation System as it have multiple functions, [14]

The set up procedure for Labview Interface for Arduino (LIFA) as below:[14]

a. Install Labview (the installer provided by supervisor)
b. Install the NI-VISA drivers
c. Install JKI VI Package Manager (VIPM) Community Edition
d. Install Labview Interface for Arduino (LIFA)
e. Connect Arduino Uno microcontroller to the laptop
f. Load the LIFA to Arduino Uno

3.1 Labview Panels

The execution of program followed the connector wires by linking the process nodes together. All of each routine or function is stored in virtual instrument (VI). The Labview consists of three main components which are front panel, block diagram and a connector panel. The panels are showed in Figure 23 and Figure 24, [14]

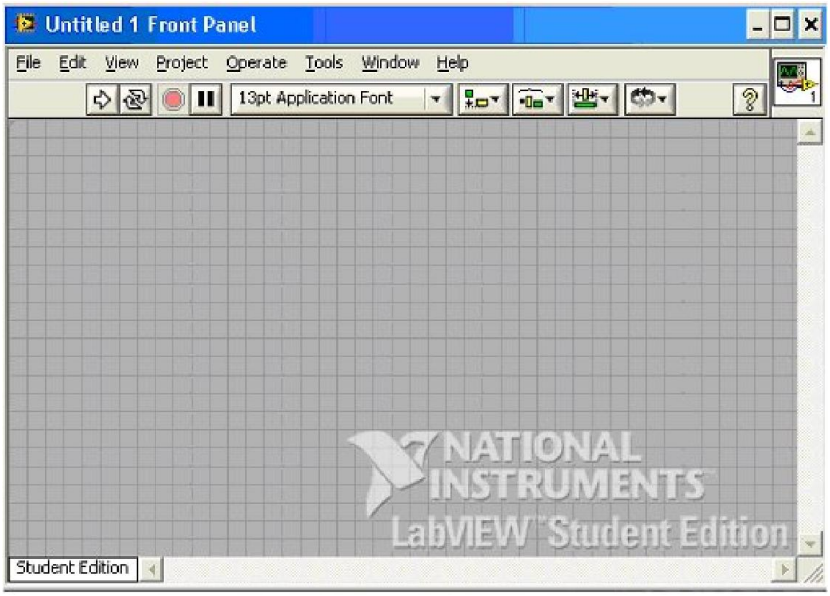

Figure 23 Front Panel of Labview

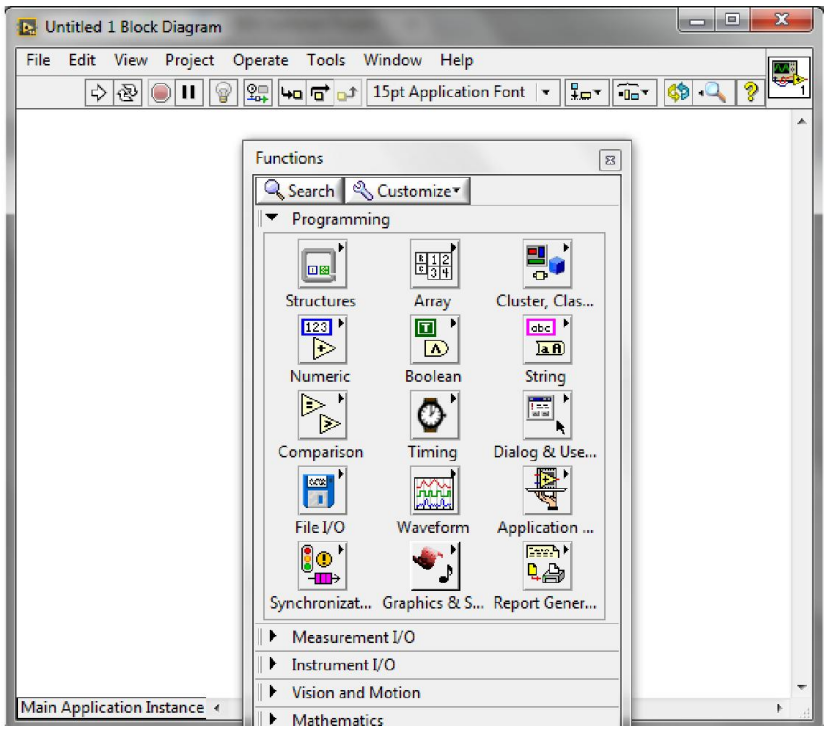

Figure 24: Block Diagram of Labview

The front panel contains inputs and controls which displayed at a run time while block diagram is a place for edit the code and represented graphically. The last panel which is connector panel helps in interface of VI when imbedded as a sub-VI [14]. Front panel of VI is the same in the web browser window as it is on the local computer. Only one user can control the VI, while others can observe the experiment from the VI or web cam live video [14].

3.2 Designing Labview for speed control of DC motor

The main part of this project is interfacing of Labview with Arduino. The designing block diagram and front panel is developed using Labview software. The design is built in order to control the speed of DC motor.

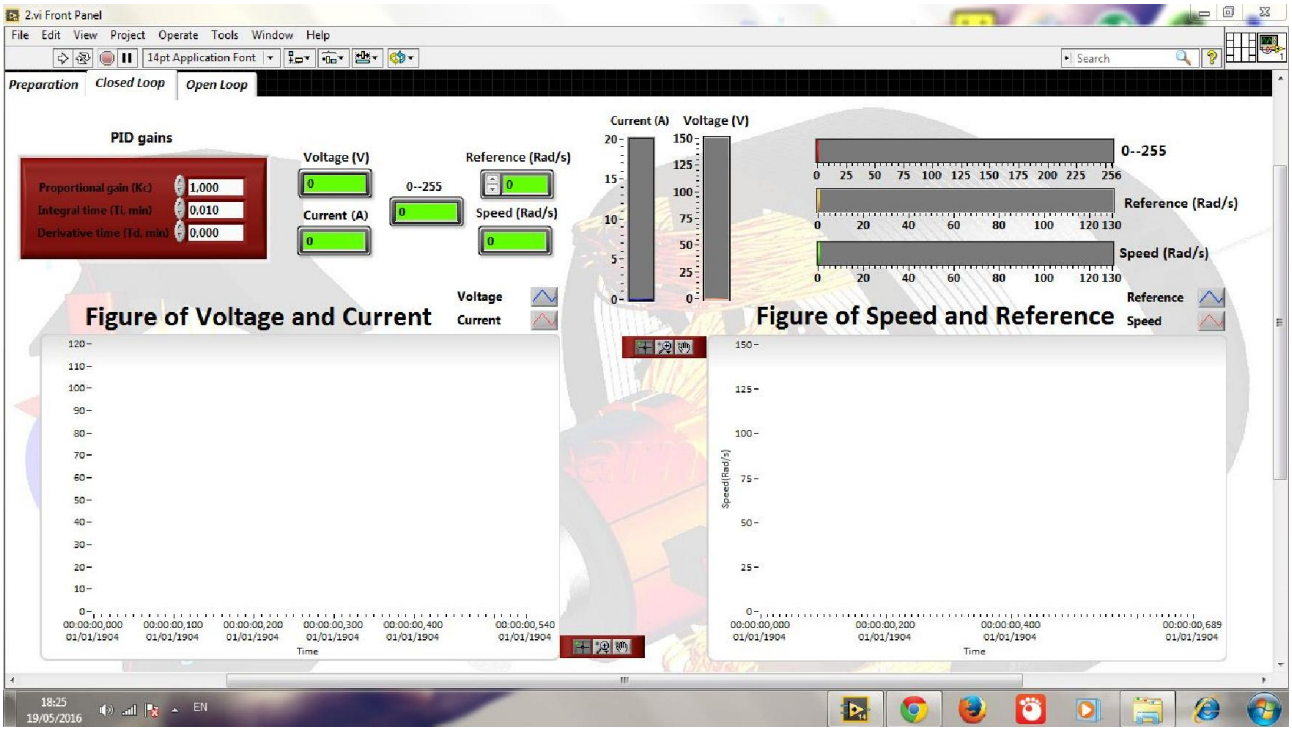

Figure 25 : Front panel for sensers

Figure 25 shows the front panels for sensers. This panel will shows the user six waveform graphs that indicate the reading value from the sensors. There is also 3 meters used in this system which are voltmeter, ampermeter and tachymeter. From this, user is able to monitor the environment condition comfortably.

Duty cycle can be varied from 0-100% by varying the user controlled interactive graphical dial on the front panel. The response of the system can be changed by varying the gains of PID controller. These VI's will be burnt in the Arduino microcontroller using LIFA_Base and interfaced with the dc motor. Setpoint, set by the user will be fed into the PID controller and passed on to the Arduino PWM pins. Arduino will pass those PWM pulses to the motor along with supply voltage that moves the motor. Shaft of the DC motor will move and number of times it moves will give us the speed at which the motor is moving. Tachometer is the sensor which measures the rotation will be used. Tachometer will be given external power supply voltage of 5V.[11]

Belows is the Block diagram of the Closed-Loop System is as shown in Figure 26:

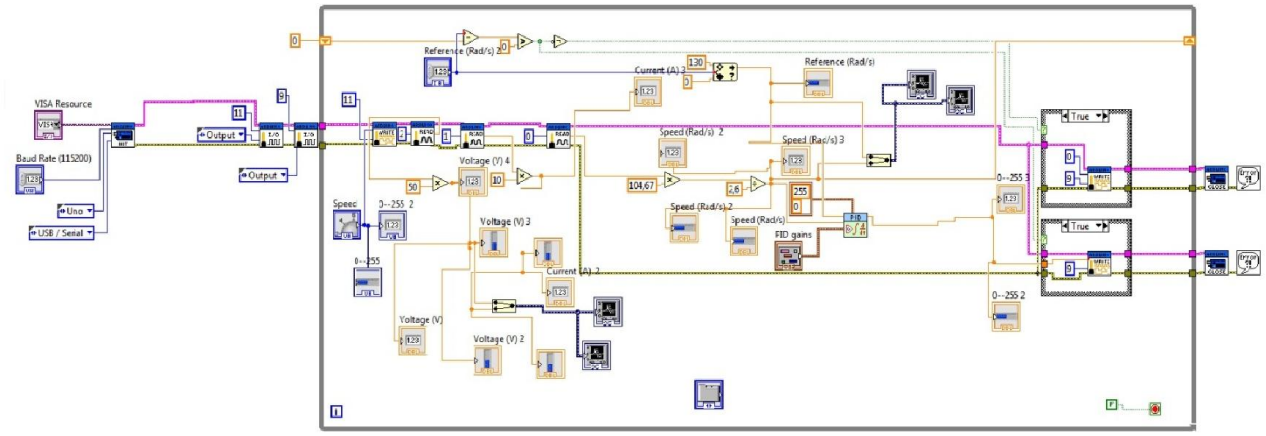

Figure 26 Block diagram of Sensors

PID controller will compare the setpoint value with the value received from the Arduino. Arduino receives this value from tachometer. Tachometer measures the revolutions of the DC motor. If the two values are not same, PID controller will try to minimize this error and bring the DC Motor to the desired speed.

4. Result and discussion

Figures 27 - 29 below shows the speed control of DC motor with PID controller. The value at which the speed is obtained at K_c=11.42, T_i=0.03 and T_d=00.

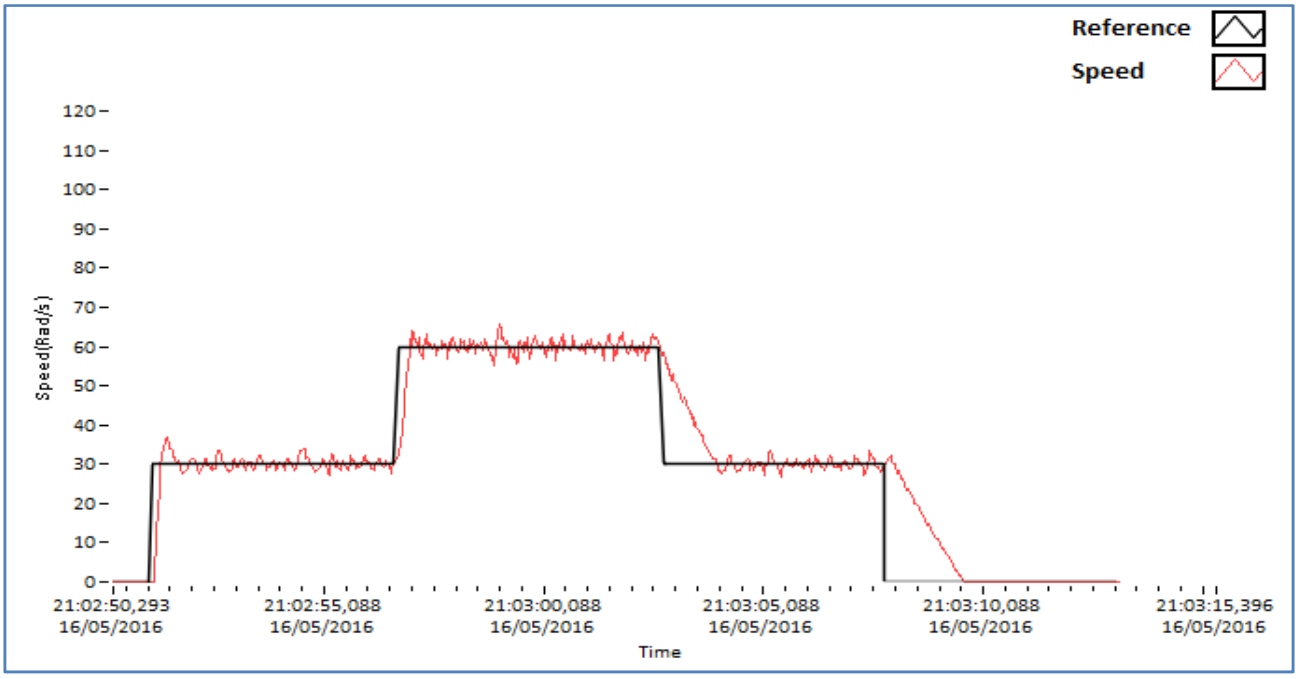

Figure 27 Speed Response with no torque load T_L=0 Nm

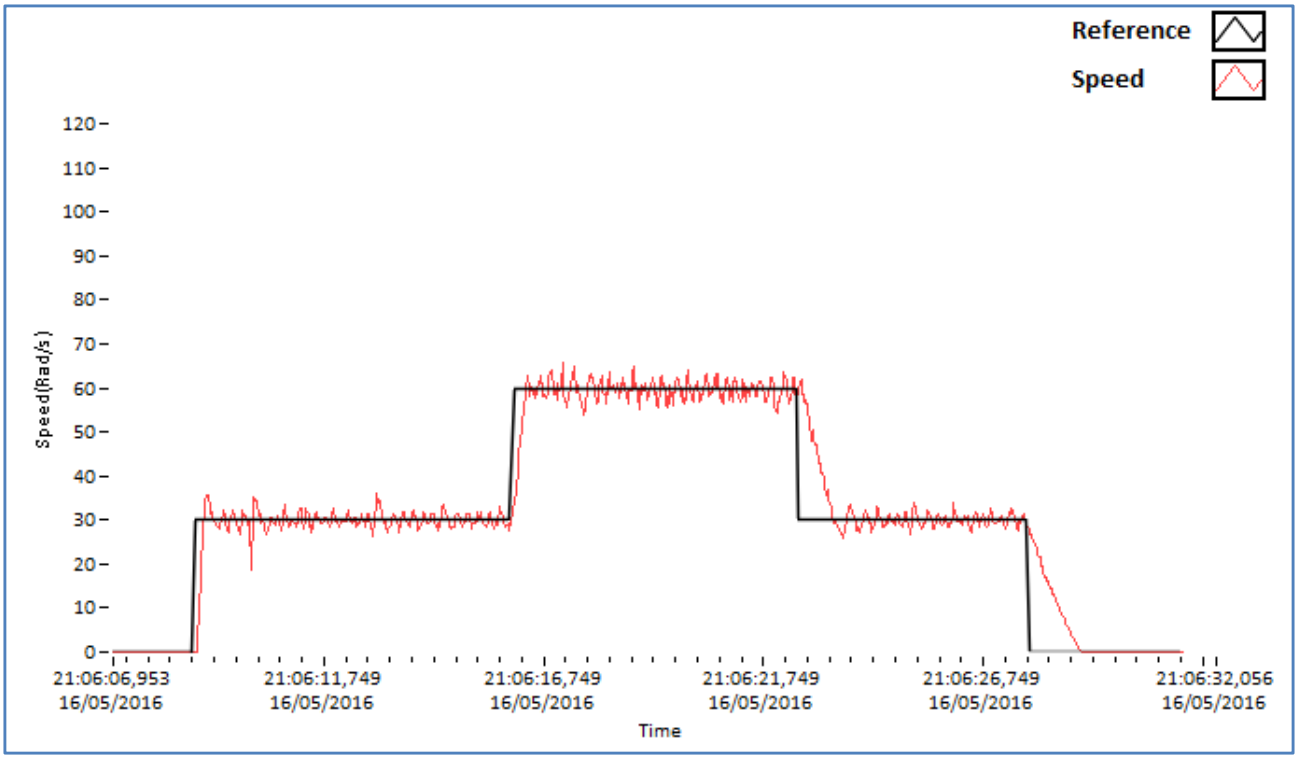

Figure 28 Speed Response with no torque load T_L=0.62 Nm

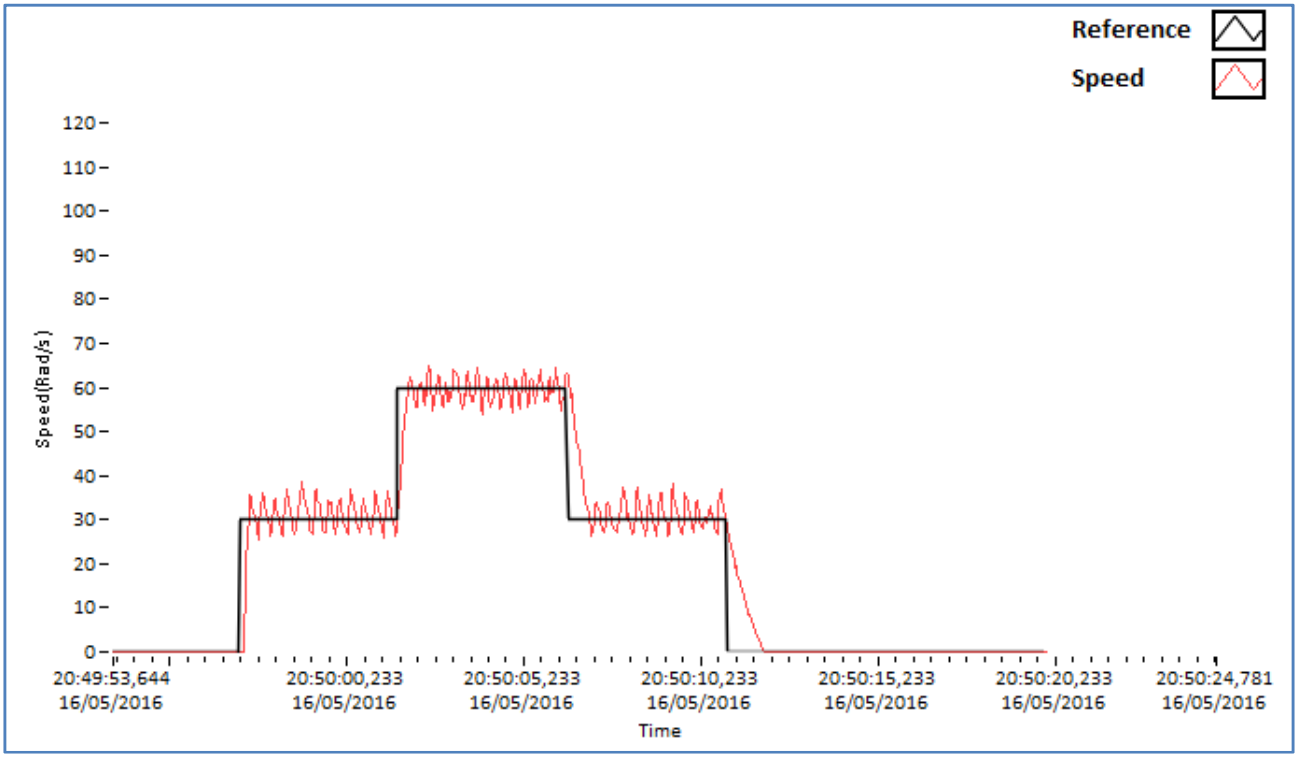

Figure 29 Speed Response with no torque load T_L= 1.35 Nm

Experimental results are shown in Fig. 27, Fig. 28 and Fig.29 for step response for speed change from 0 rad/sec to 30 rad/sec to 60 rad/sec and from 60 rad/sec to 30 rad/sec to 0 rad/sec at different

of rated motor load. These figures clarify the soft start of the motor and the operation of the current limit as well as the satisfactory transient response.

The speed of a DC motor has been successfully controlled by using Chopper as a converter and PID type Speed controller based on closed loop system model. Initially a simplified closed loop model for speed control of DC motor is considered and requirement of speed controller is studied. Then a generalized modeling of dc motor is done. After that a complete layout of DC drive system is obtained. Then designing of speed controller is done. The optimization of speed control loop is achieved through Ziegler-Nichols methode. A DC motor specification is taken and corresponding parameters are found out from derived design approach. The expermental results under varying reference speed and varying load are shown above. The test shows good results under all conditions employed during simulation.

1. Conclusion

Electric motors are used to provide mechanical work in industries. The DC motors is considered to be a basic electric machine. The DC motors are one of the electrical drives that are rapidly gaining popularity, due to their high efficiency, good dynamic response and low maintenance. The DC motors and drives have grown significantly in recent years in the appliance industry and the automotive industry. DC drives are very preferable for compact, low maintenance, and high reliability system [17].

In this work, an overview of DC motors, including the equations that represent torque, rotor speed, field and armature currents and voltages is developed. Identification and PID Controller of a 1st Order DC Motor Model is discussed. The Results of the testing about the Speed Control of DC Motor performance are analyzed. A PID controller has been employed for speed control of DC motor by LabView interfaced with Arduino. The speed controller has been designed successfully for closed loop operation of the DC motor and the motor runs nearly to the reference speed. The expermental results under varying reference speed and varying load are shown above. The test shows good results under all conditions employed during simulation.

2. Future Scope

- Tuning of PID controller for position control using Artificial Intelligence techniques such as : Neural Network and Fuzzy approach …
- Speed control of the DC motor for shunt-connected, series-connected, or compound-connected operation.

References

[1] Mohamed farid bin mohamed faruq , pid controller design for controlling dc motor speed using matlab application, Thesis of Master, universiti malaysia pahang, nov. 2008.

[2] Amir Faizy, Shailendra Kumar, "Dc Motor Control Using Chopper" Thesis Of Master , National Institute Of Technology, 2013.

[3] Waleed Ahmed Mohammed Hussein Ahmed , PID Control of DC-Motors, Thesis Of Master , University of Khartoum, 2003,

[4] Jonathan r. derges, torque control of a separate-winding excitation dc motor for a dynamometer, thesis of master, naval postgraduate school, 2010

[5] http://www.electrical4u.com/types-of-dc-motor-separately-excited-shunt-series-compound-dc-motor/

[6] Bassim M. H. Jassim, Tagreed M. Ali Modeling and Simulation of Sensorless Speed Control of a Buck Converter Controlled Dc Motor, Al-Khwarizmi Engineering Journal, Vol. 6, No. 1, PP 80 - 87 (2010).

[7] http://www.mathworks.com/help/physmod/sps/powersys/ref/onequadrantchopper-dcdrive.html.

[8] Ned mohan, tore m. undeland, william p. robbins" power electronics Converters, Applications, and Design; 2003.

[9] http://www.electrical4u.com/chopper-dc-to-dc-converter/

[10] http://www.talkingelectronics.com/projects/MOSFET/MOSFET.html

[11] Pratap Vikhe, Neelam Punjabi, Chandrakant Kadu Real Time DC Motor Speed Control using PID Controller in LabVIEW, International Journal of Advanced Research in Electrical, Electronics and Instrumentation Engineering, Vol. 3, Issue 9, September 2014.

[12] Modeling and Experimental Validation of a First Order Plant Model: DC Servo Motor.

[13] Tan Kok Kiong, Wang Qing-Guo, Hang Chang Chieh , Advances in Industrial Control, Lund University.

[14] Nik Syarifah Nurhidayah Binti Nik Fauzi , An Automatic Fertigation System Using Labview And Arduino, Universiti Teknologi Malaysia. Thesis of Master, 2014/2015.

[15] http://emadrlc.blogspot.com/2012/07/dc-motor-field-structure-and-armature.html.

[16] http://electrical-engineering-portal.com/basics-of-dc-motors-for-electrical-engineers-beginners.

[17] MohdZeeshanHaider, Position Control of Permanent Magnet Brushless DC Motor using PID Controller, Master of Engineering, Thapar University, Patiala, 2011.

FAIRCHILD
SEMICONDUCTOR®

GENERAL PURPOSE 6-PIN PHOTOTRANSISTOR OPTOCOUPLERS

4N25	4N26	4N27	4N28	4N35	4N36
4N37	H11A1	H11A2	H11A3	H11A4	H11A5

WHITE PACKAGE (-M SUFFIX)

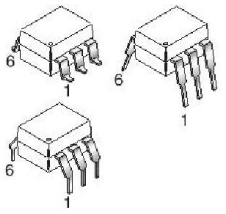

SCHEMATIC

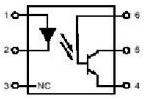

PIN 1. ANODE
2. CATHODE
3. NO CONNECTION
4. EMITTER
5. COLLECTOR
6. BASE

BLACK PACKAGE (NO -M SUFFIX)

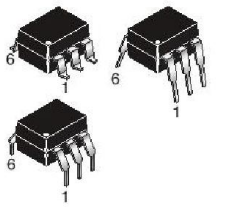

DESCRIPTION

The general purpose optocouplers consist of a gallium arsenide infrared emitting diode driving a silicon phototransistor in a 6-pin dual in-line package.

FEATURES

- Also available in white package by specifying -M suffix, eg. 4N25-M
- UL recognized (File # E90700)
- VDE recognized (File # 94766)
  - Add option V for white package (e.g., 4N25V-M)
  - Add option 300 for black package (e.g., 4N25.300)

APPLICATIONS

- Power supply regulators
- Digital logic inputs
- Microprocessor inputs

FAIRCHILD SEMICONDUCTOR®

GENERAL PURPOSE 6-PIN PHOTOTRANSISTOR OPTOCOUPLERS

4N25	4N26	4N27	4N28	4N35	4N36
4N37	H11A1	H11A2	H11A3	H11A4	H11A5

ABSOLUTE MAXIMUM RATINGS (T_A = 25°C unless otherwise specified)

Parameter	Symbol	Value	Units
TOTAL DEVICE			
Storage Temperature	T_{STG}	-55 to +150	°C
Operating Temperature	T_{OPR}	-55 to +100	°C
Wave solder temperature (see page 14 for reflow solder profiles)	T_{SOL}	260 for 10 sec	°C
Total Device Power Dissipation @ T_A = 25°C	P_D	250	mW
Derate above 25°C		3.3 (non-M), 2.94 (-M)	
EMITTER			
DC/Average Forward Input Current	I_F	100 (non-M), 60 (-M)	mA
Reverse Input Voltage	V_R	6	V
Forward Current - Peak (300µs, 2% Duty Cycle)	I_F(pk)	3	A
LED Power Dissipation @ T_A = 25°C	P_D	150 (non-M), 120 (-M)	mW
Derate above 25°C		2.0 (non-M), 1.41 (-M)	mW/°C
DETECTOR			
Collector-Emitter Voltage	V_{CEO}	30	V
Collector-Base Voltage	V_{CBO}	70	V
Emitter-Collector Voltage	V_{ECO}	7	V
Detector Power Dissipation @ T_A = 25°C	P_D	150	mW
Derate above 25°C		2.0 (non-M), 1.76 (-M)	mW/°C

FAIRCHILD SEMICONDUCTOR®

GENERAL PURPOSE 6-PIN PHOTOTRANSISTOR OPTOCOUPLERS

4N25	4N26	4N27	4N28	4N35	4N36
4N37	H11A1	H11A2	H11A3	H11A4	H11A5

ELECTRICAL CHARACTERISTICS (T_A = 25°C unless otherwise specified)

INDIVIDUAL COMPONENT CHARACTERISTICS

Parameter	Test Conditions	Symbol	Min	Typ*	Max	Unit
EMITTER						
Input Forward Voltage	(I_F = 10 mA)	V_F		1.18	1.50	V
Reverse Leakage Current	(V_R = 6.0 V)	I_R		0.001	10	µA
DETECTOR						
Collector-Emitter Breakdown Voltage	(I_C = 1.0 mA, I_F = 0)	BV_{CEO}	30	100		V
Collector-Base Breakdown Voltage	(I_C = 100 µA, I_F = 0)	BV_{CBO}	70	120		V
Emitter-Collector Breakdown Voltage	(I_E = 100 µA, I_F = 0)	BV_{ECO}	7	10		V
Collector-Emitter Dark Current	(V_{CE} = 10 V, I_F = 0)	I_{CEO}		1	50	nA
Collector-Base Dark Current	(V_{CB} = 10 V)	I_{CBO}			20	nA
Capacitance	(V_{CE} = 0 V, f = 1 MHz)	C_{CE}		8		pF

ISOLATION CHARACTERISTICS

Characteristic	Test Conditions	Symbol	Min	Typ*	Max	Units
Input-Output Isolation Voltage	(Non '-M', Black Package) (f = 60 Hz, t = 1 min)	V_{ISO}	5300			Vac(rms)
	('-M', White Package) (f = 60 Hz, t = 1 sec)		7500			Vac(pk)
Isolation Resistance	(V_{I-O} = 500 VDC)	R_{ISO}	10^{11}			Ω
Isolation Capacitance	(V_{I-O} = &, f = 1 MHz)	C_{ISO}		0.5		pF
	('-M' White Package)			0.2	2	pF

Note
* Typical values at T_A = 25°C

FAIRCHILD SEMICONDUCTOR®

GENERAL PURPOSE 6-PIN PHOTOTRANSISTOR OPTOCOUPLERS

4N25	4N26	4N27	4N28	4N35	4N36
4N37	H11A1	H11A2	H11A3	H11A4	H11A5

TRANSFER CHARACTERISTICS (T_A = 25°C Unless otherwise specified.)

DC Characteristic	Test Conditions	Symbol	Device	Min	Typ*	Max	Unit
Current Transfer Ratio, Collector to Emitter	(I_F = 10 mA, V_{CE} = 10 V)	CTR	4N35 4N36 4N37	100			%
			H11A1	50			
			H11A5	30			
			4N25 4N26 H11A2 H11A3	20			
			4N27 4N28 H11A4	10			
	(I_F = 10 mA, V_{CE} = 10 V, T_A = -55°C)		4N35 4N36 4N37	40			
	(I_F = 10 mA, V_{CE} = 10 V, T_A = +100°C)		4N35 4N36 4N37	40			
Collector-Emitter Saturation Voltage	(I_C = 2 mA, I_F = 50 mA)	$V_{CE\ (SAT)}$	4N25 4N26 4N27 4N28			0.5	V
	(I_C = 0.5 mA, I_F = 10 mA)		4N35 4N36 4N37			0.3	
			H11A1 H11A2 H11A3 H11A4 H11A5			0.4	
AC Characteristic Non-Saturated Turn-on Time	(I_F = 10 mA, V_{CC} = 10 V, R_L = 100Ω) (Fig.20)	T_{ON}	4N25 4N26 4N27 4N28 H11A1 H11A2 H11A3 H11A4 H11A5		2		µs
Non Saturated Turn-on Time	(I_C = 2 mA, V_{CC} = 10 V, R_L = 100Ω) (Fig.20)	T_{ON}	4N35 4N36 4N37		2	10	µs

FAIRCHILD SEMICONDUCTOR®

GENERAL PURPOSE 6-PIN PHOTOTRANSISTOR OPTOCOUPLERS

4N25	4N26	4N27	4N28	4N35	4N36
4N37	H11A1	H11A2	H11A3	H11A4	H11A5

TRANSFER CHARACTERISTICS (T_A = 25°C Unless otherwise specified.) (Continued)

AC Characteristic	Test Conditions	Symbol	Device	Min	Typ*	Max	Unit
Turn-off Time	(I_F = 10 mA, V_{CC} = 10 V, R_L = 100Ω) (Fig.20)	T_{OFF}	4N25 4N26 4N27 4N28 H11A1 H11A2 H11A3 H11A4 H11A5		2		µs
	(I_C = 2 mA, V_{CC} = 10 V, R_L = 100Ω) (Fig.20)		4N35 4N36 4N37		2	10	

* Typical values at T_A = 25°C

FAIRCHILD SEMICONDUCTOR®

GENERAL PURPOSE 6-PIN PHOTOTRANSISTOR OPTOCOUPLERS

4N25	4N26	4N27	4N28	4N35	4N36
4N37	H11A1	H11A2	H11A3	H11A4	H11A5

TYPICAL PERFORMANCE CURVES

Fig. 1 LED Forward Voltage vs. Forward Current (Black Package)

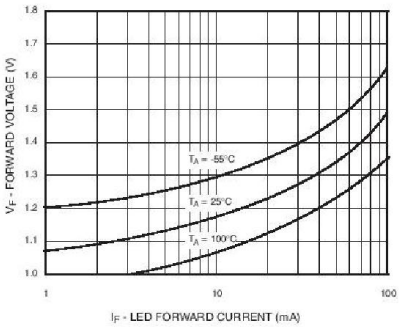

Fig. 2 LED Forward Voltage vs. Forward Current (White Package)

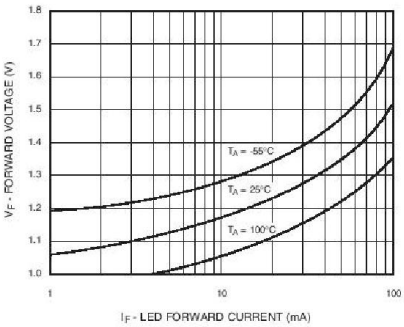

Fig.3 Normalized CTR vs. Forward Current (Black Package)

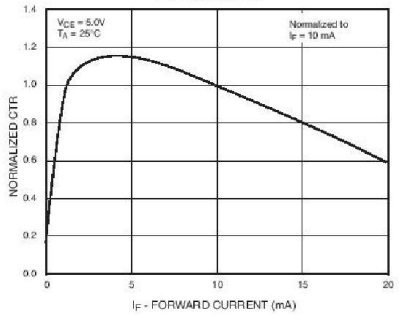

Fig.4 Normalized CTR vs. Forward Current (White Package)

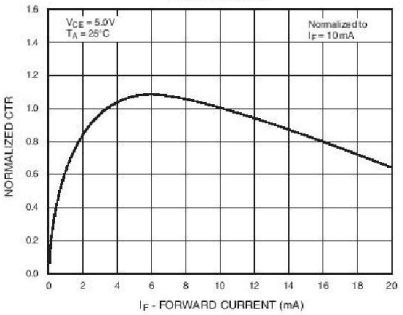

Fig. 5 Normalized CTR vs. Ambient Temperature (Black Package)

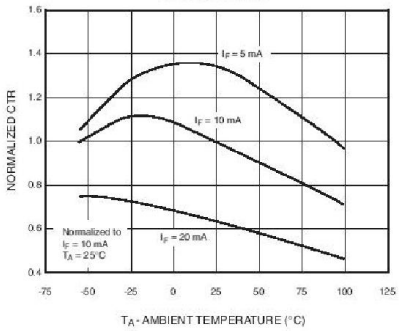

Fig. 6 Normalized CTR vs. Ambient Temperature (White Package)

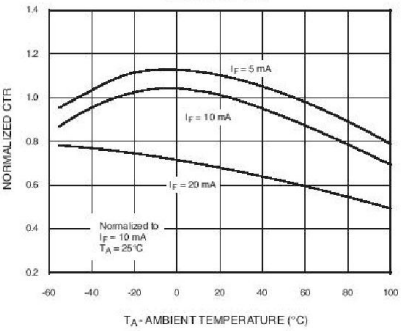

FAIRCHILD SEMICONDUCTOR®

GENERAL PURPOSE 6-PIN PHOTOTRANSISTOR OPTOCOUPLERS

4N25 4N37	4N26 H11A1	4N27 H11A2	4N28 H11A3	4N35 H11A4	4N36 H11A5

Fig. 7 CTR vs. RBE (Unsaturated) (Black Package)

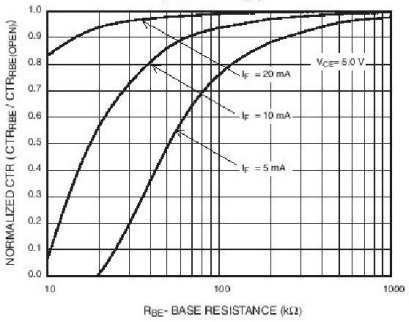

Fig. 8 CTR vs. RBE (Unsaturated) (White Package)

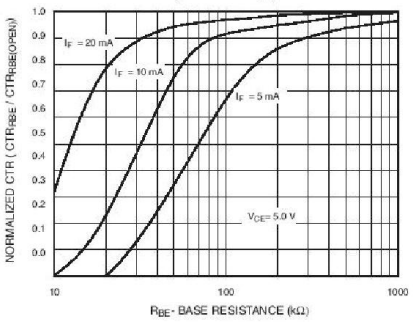

Fig. 9 CTR vs. RBE (Saturated) (Black Package)

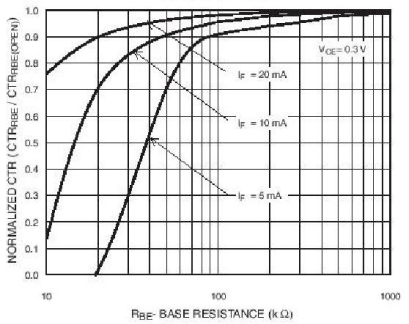

Fig. 10 CTR vs. RBE (Saturated) (White Package)

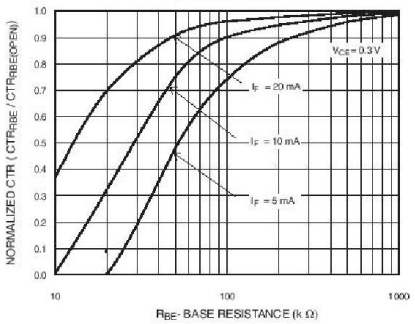

Fig. 11 Collector-Emitter Saturation Voltage vs Collector Current (Black Package)

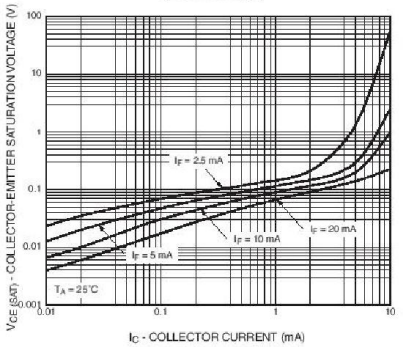

Fig. 12 Collector-Emitter Saturation Voltage vs Collector Current (White Package)

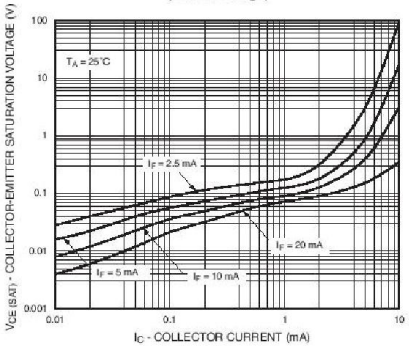

FAIRCHILD SEMICONDUCTOR®

GENERAL PURPOSE 6-PIN PHOTOTRANSISTOR OPTOCOUPLERS

4N25 4N37	4N26 H11A1	4N27 H11A2	4N28 H11A3	4N35 H11A4	4N36 H11A5

Fig. 13 Switching Speed vs. Load Resistor (Black Package)

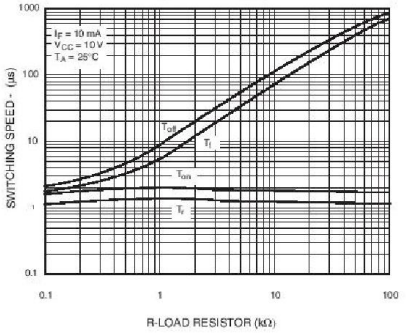

Fig. 14 Switching Speed vs. Load Resistor (White Package)

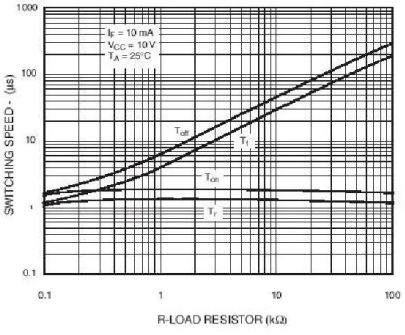

Fig. 15 Normalized t_{on} vs. R_{BE} (Black Package)

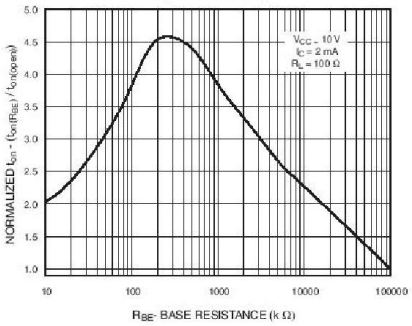

Fig. 16 Normalized t_{on} vs. R_{BE} (White Package)

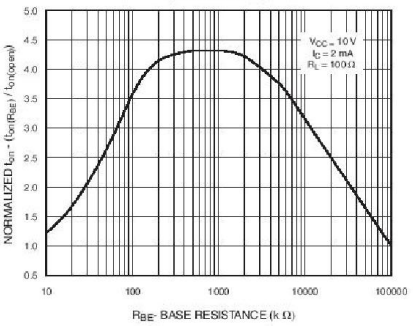

Fig. 17 Normalized t_{off} vs. R_{BE} (Black Package)

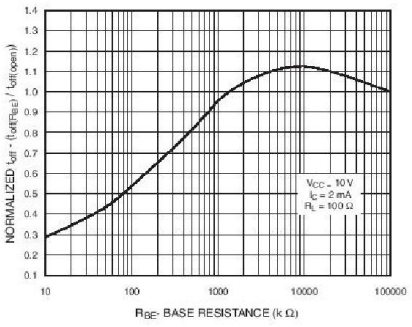

Fig. 18 Normalized t_{off} vs. R_{BE} (White Package)

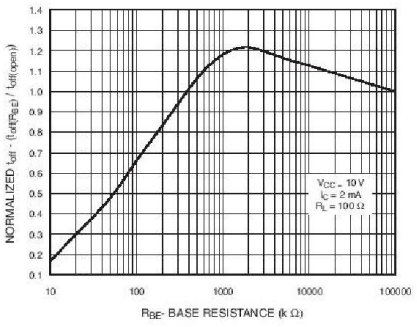

FAIRCHILD SEMICONDUCTOR®

GENERAL PURPOSE 6-PIN PHOTOTRANSISTOR OPTOCOUPLERS

4N25	4N26	4N27	4N28	4N35	4N36
4N37	H11A1	H11A2	H11A3	H11A4	H11A5

Fig. 19 Dark Current vs. Ambient Temperature

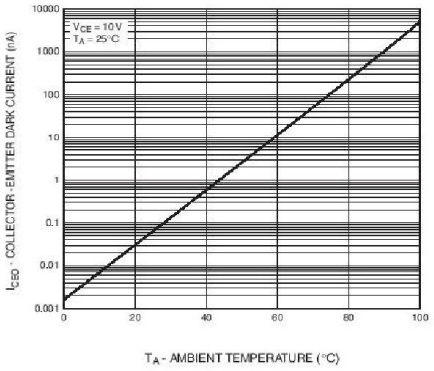

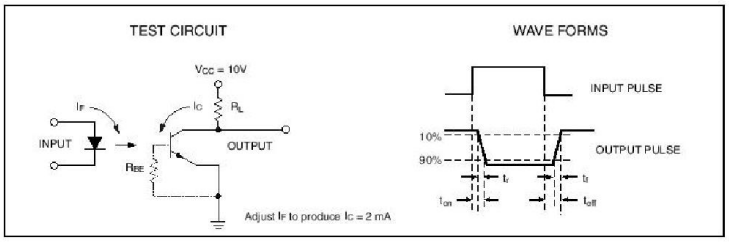

Figure 20. Switching Time Test Circuit and Waveforms

FAIRCHILD SEMICONDUCTOR®

GENERAL PURPOSE 6-PIN PHOTOTRANSISTOR OPTOCOUPLERS

4N25	4N26	4N27	4N28	4N35	4N36
4N37	H11A1	H11A2	H11A3	H11A4	H11A5

Black Package (No -M Suffix)

Package Dimensions (Through Hole)

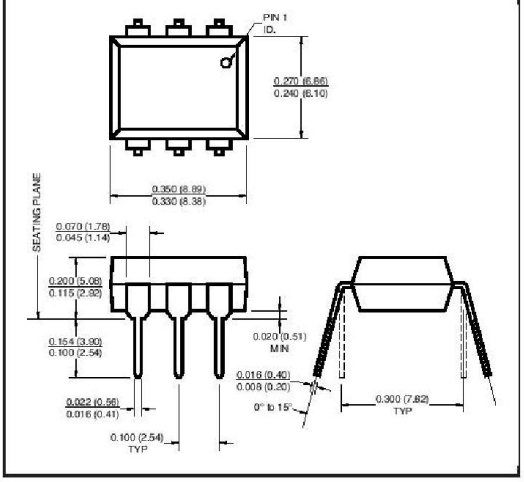

Package Dimensions (Surface Mount)

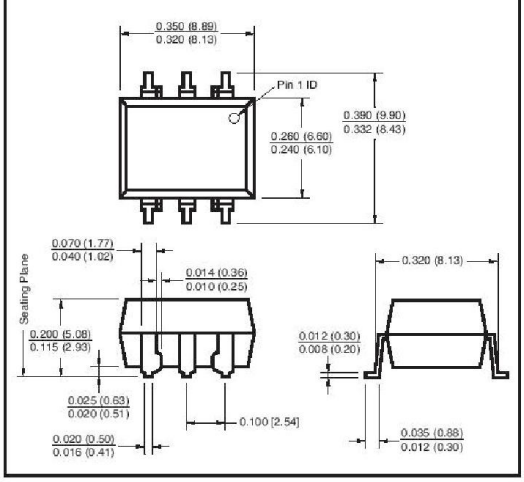

Package Dimensions (0.4" Lead Spacing)

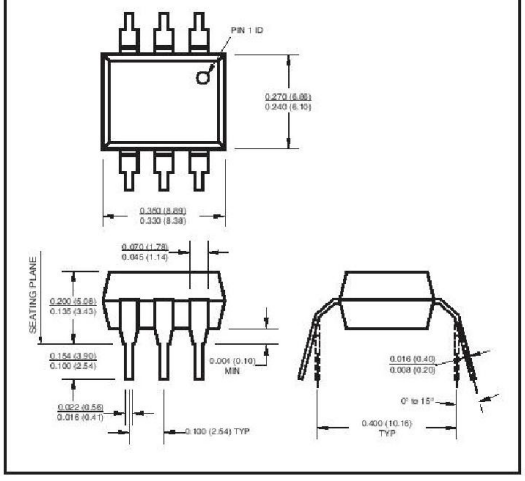

Recommended Pad Layout for Surface Mount Leadform

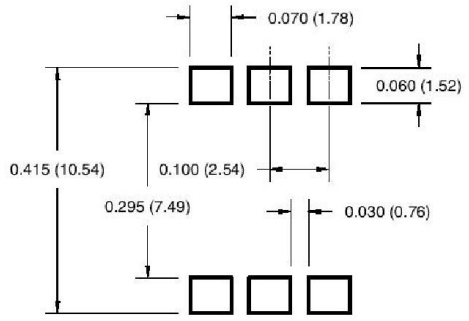

NOTE
All dimensions are in inches (millimeters)

FAIRCHILD SEMICONDUCTOR®

GENERAL PURPOSE 6-PIN PHOTOTRANSISTOR OPTOCOUPLERS

4N25	4N26	4N27	4N28	4N35	4N36
4N37	H11A1	H11A2	H11A3	H11A4	H11A5

White Package (-M Suffix)

Package Dimensions (Through Hole)

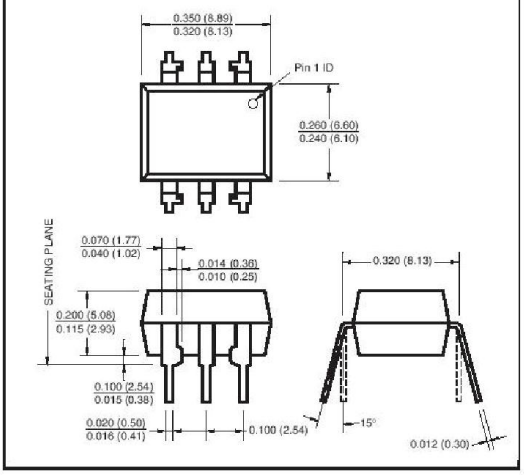

Package Dimensions (Surface Mount)

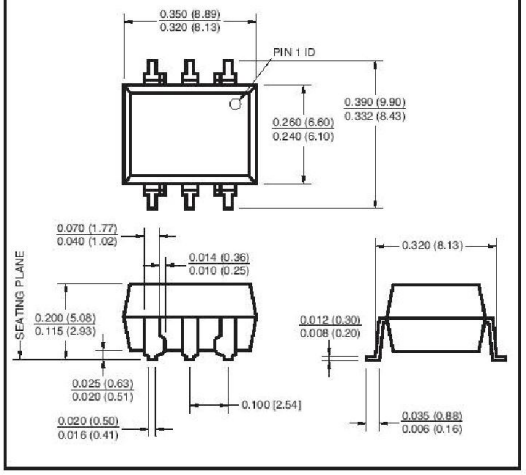

Package Dimensions (0.4" Lead Spacing)

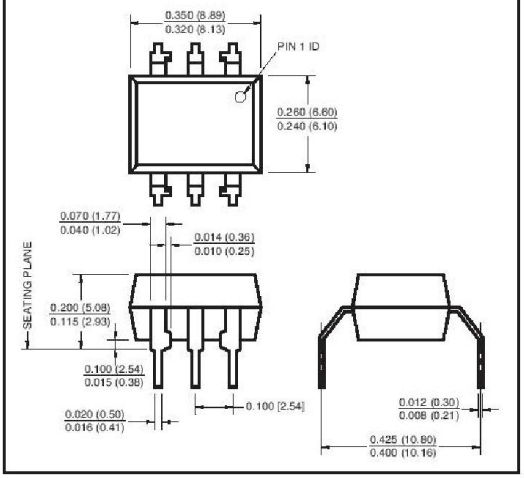

Recommended Pad Layout for Surface Mount Leadform

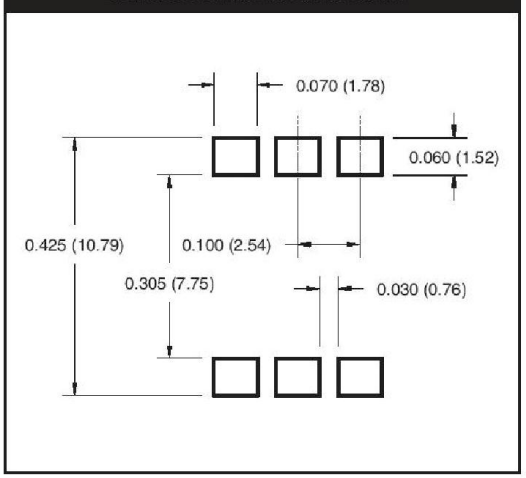

NOTE
All dimensions are in inches (millimeters)

FAIRCHILD SEMICONDUCTOR®

GENERAL PURPOSE 6-PIN PHOTOTRANSISTOR OPTOCOUPLERS

4N25	4N26	4N27	4N28	4N35	4N36
4N37	H11A1	H11A2	H11A3	H11A4	H11A5

ORDERING INFORMATION

Order Entry Identifier		
Black Package (No Suffix)	**White Package (-M Suffix)**	**Option**
.S	S	Surface Mount Lead Bend
.SD	SR2	Surface Mount; Tape and reel
.W	T	0.4" Lead Spacing
.300	V	VDE 0884
.300W	TV	VDE 0884, 0.4" Lead Spacing
.3S	SV	VDE 0884, Surface Mount
.3SD	SR2V	VDE 0884, Surface Mount, Tape & Reel

MARKING INFORMATION

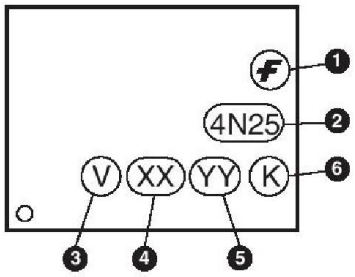

Black Package, No Suffix

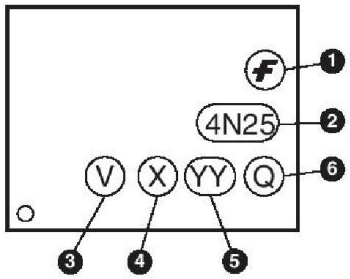

White Package, -M Suffix

Definitions	
1	Fairchild logo
2	Device number
3	VDE mark (Note: Only appears on parts ordered with VDE option – See order entry table)
4	One or two digit year code • Two digits for black package parts, e.g., '03' • One digit for white package parts, e.g., '3'
5	Two digit work week ranging from '01' to '53'
6	Assembly package code

*Note – Parts built in the white package (M suffix) that do not have the 'V' option (see definition 3 above) that are marked with date code '325' or earlier are marked in the portrait format.

FAIRCHILD SEMICONDUCTOR®

GENERAL PURPOSE 6-PIN PHOTOTRANSISTOR OPTOCOUPLERS

4N25	4N26	4N27	4N28	4N35	4N36
4N37	H11A1	H11A2	H11A3	H11A4	H11A5

QT Carrier Tape Specifications (Black Package, No Suffix)

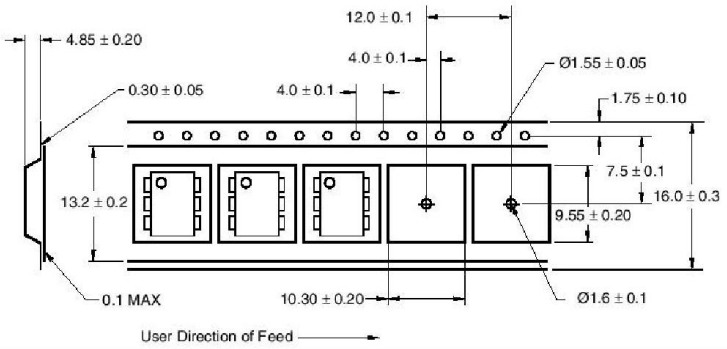

QT Carrier Tape Specifications (White Package, -M Suffix)

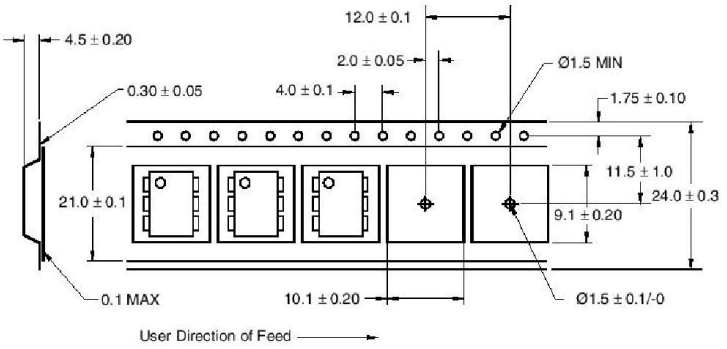

FAIRCHILD SEMICONDUCTOR®

GENERAL PURPOSE 6-PIN PHOTOTRANSISTOR OPTOCOUPLERS

4N25	4N26	4N27	4N28	4N35	4N36
4N37	H11A1	H11A2	H11A3	H11A4	H11A5

Reflow Profile (White Package, -M Suffix)

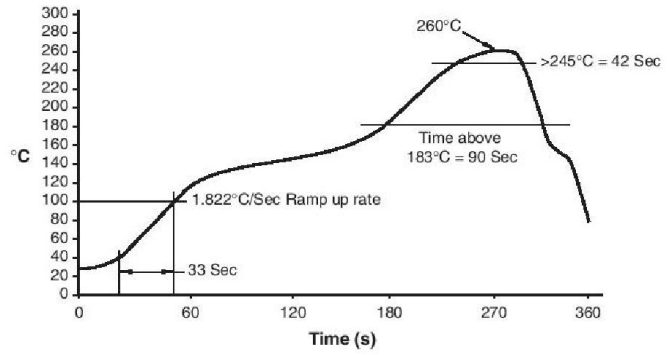

Reflow Profile (Black Package, No Suffix)

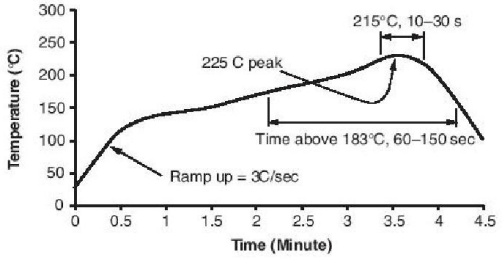

- Peak reflow temperature: 225°C (package surface temperature)
- Time of temperature higher than 183°C for 60–150 seconds
- One time soldering reflow is recommended

FAIRCHILD SEMICONDUCTOR®

GENERAL PURPOSE 6-PIN PHOTOTRANSISTOR OPTOCOUPLERS

4N25	4N26	4N27	4N28	4N35	4N36
4N37	H11A1	H11A2	H11A3	H11A4	H11A5

FAIRCHILD SEMICONDUCTOR®

IGBT

SGH40N60UFD

Ultra-Fast IGBT

General Description

Fairchild's UFD series of Insulated Gate Bipolar Transistors (IGBTs) provides low conduction and switching losses. The UFD series is designed for applications such as motor control and general inverters where high speed switching is a required feature.

Features

- High speed switching
- Low saturation voltage : $V_{CE(sat)}$ = 2.1 V @ I_C = 20A
- High input impedance
- CO-PAK, IGBT with FRD : t_{rr} = 42ns (typ.)

Applications

AC & DC motor controls, general purpose inverters, robotics, and servo controls.

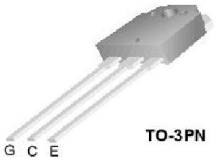

TO-3PN

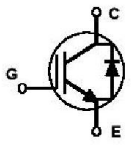

Absolute Maximum Ratings

T_C = 25°C unless otherwise noted

Symbol	Description		SGH40N60UFD	Units
V_{CES}	Collector-Emitter Voltage		600	V
V_{GES}	Gate-Emitter Voltage		± 20	V
I_C	Collector Current	@ T_C = 25°C	40	A
	Collector Current	@ T_C = 100°C	20	A
$I_{CM\ (1)}$	Pulsed Collector Current		160	A
I_F	Diode Continuous Forward Current	@ T_C = 100°C	15	A
I_{FM}	Diode Maximum Forward Current		160	A
P_D	Maximum Power Dissipation	@ T_C = 25°C	160	W
	Maximum Power Dissipation	@ T_C = 100°C	64	W
T_J	Operating Junction Temperature		-55 to +150	°C
T_{stg}	Storage Temperature Range		-55 to +150	°C
T_L	Maximum Lead Temp. for Soldering Purposes, 1/8" from Case for 5 Seconds		300	°C

Notes :
(1) Repetitive rating : Pulse width limited by max. junction temperature

Thermal Characteristics

Symbol	Parameter	Typ.	Max.	Units
$R_{\theta JC}$(IGBT)	Thermal Resistance, Junction-to-Case	–	0.77	°C/W
$R_{\theta JC}$(DIODE)	Thermal Resistance, Junction-to-Case	–	1.7	°C/W
$R_{\theta JA}$	Thermal Resistance, Junction-to-Ambient	–	40	°C/W

Electrical Characteristics of the IGBT T_C = 25°C unless otherwise noted

Symbol	Parameter	Test Conditions	Min.	Typ.	Max.	Units
Off Characteristics						
BV_{CES}	Collector-Emitter Breakdown Voltage	V_{GE} = 0V, I_C = 250uA	600	–	–	V
$\Delta B_{VCES}/\Delta T_J$	Temperature Coefficient of Breakdown Voltage	V_{GE} = 0V, I_C = 1mA	--	0.6	–	V/°C
I_{CES}	Collector Cut-Off Current	V_{CE} = V_{CES}, V_{GE} = 0V	--	--	250	uA
I_{GES}	G-E Leakage Current	V_{GE} = V_{GES}, V_{CE} = 0V	--	--	±100	nA
On Characteristics						
$V_{GE(th)}$	G-E Threshold Voltage	I_C = 20mA, V_{CE} = V_{GE}	3.5	4.5	6.5	V
$V_{CE(sat)}$	Collector to Emitter Saturation Voltage	I_C = 20A, V_{GE} = 15V	--	2.1	2.6	V
		I_C = 40A, V_{GE} = 15V	--	2.6	–	V
Dynamic Characteristics						
C_{ies}	Input Capacitance	V_{CE} = 30V, V_{GE} = 0V, f = 1MHz	--	1430	–	pF
C_{oes}	Output Capacitance		--	170	–	pF
C_{res}	Reverse Transfer Capacitance		--	50	–	pF
Switching Characteristics						
$t_{d(on)}$	Turn-On Delay Time	V_{CC} = 300 V, I_C = 20A, R_G = 10Ω, V_{GE} = 15V, Inductive Load, T_C = 25°C	--	15	–	ns
t_r	Rise Time		--	30	–	ns
$t_{d(off)}$	Turn-Off Delay Time		--	65	130	ns
t_f	Fall Time		--	50	150	ns
E_{on}	Turn-On Switching Loss		--	160	–	uJ
E_{off}	Turn-Off Switching Loss		--	200	–	uJ
E_{ts}	Total Switching Loss		--	360	600	uJ
$t_{d(on)}$	Turn-On Delay Time	V_{CC} = 300 V, I_C = 20A, R_G = 10Ω, V_{GE} = 15V, Inductive Load, T_C = 125°C	--	30	–	ns
t_r	Rise Time		--	37	–	ns
$t_{d(off)}$	Turn-Off Delay Time		--	110	200	ns
t_f	Fall Time		--	144	250	ns
E_{on}	Turn-On Switching Loss		--	310	–	uJ
E_{off}	Turn-Off Switching Loss		--	430	–	uJ
E_{ts}	Total Switching Loss		--	740	1200	uJ
Q_g	Total Gate Charge	V_{CE} = 300 V, I_C = 20A, V_{GE} = 15V	--	97	150	nC
Q_{ge}	Gate-Emitter Charge		--	20	30	nC
Q_{gc}	Gate-Collector Charge		--	25	40	nC
L_e	Internal Emitter Inductance	Measured 5mm from PKG	--	14	–	nH

Electrical Characteristics of DIODE T_C = 25°C unless otherwise noted

Symbol	Parameter	Test Conditions		Min.	Typ.	Max.	Units
V_{FM}	Diode Forward Voltage	I_F = 15A	T_C = 25°C	–	1.4	1.7	V
			T_C = 100°C	–	1.3	–	
t_{rr}	Diode Reverse Recovery Time	I_F = 15A, di/dt = 200A/us	T_C = 25°C	–	42	60	ns
			T_C = 100°C	–	74	–	
I_{rr}	Diode Peak Reverse Recovery Current		T_C = 25°C	–	4.5	6.0	A
			T_C = 100°C	–	6.5	–	
Q_{rr}	Diode Reverse Recovery Charge		T_C = 25°C	–	80	180	nC
			T_C = 100°C	–	220	–	

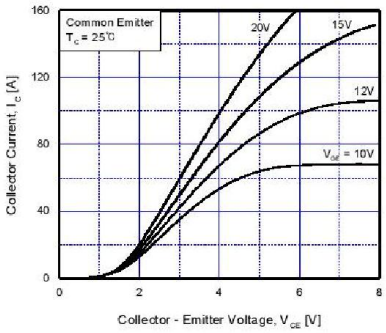

Fig 1. Typical Output Characteristics

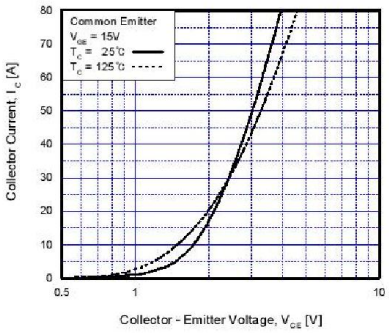

Fig 2. Typical Saturation Voltage Characteristics

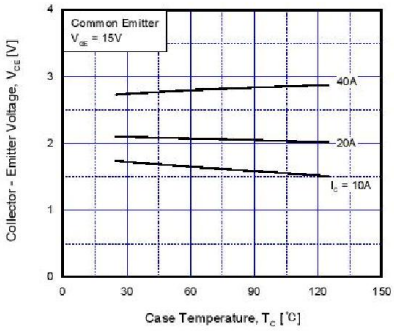

Fig 3. Saturation Voltage vs. Case Temperature at Variant Current Level

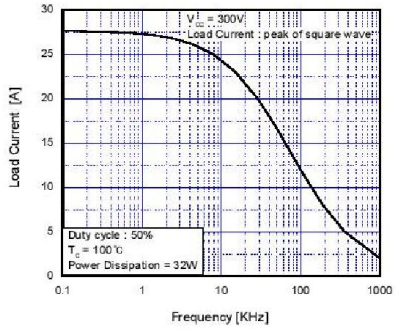

Fig 4. Load Current vs. Frequency

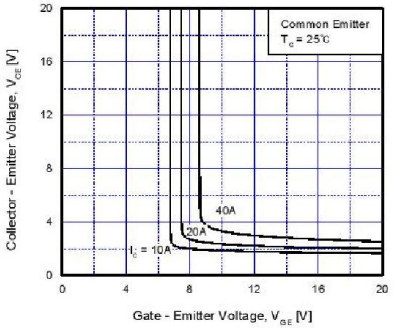

Fig 5. Saturation Voltage vs. V_{GE}

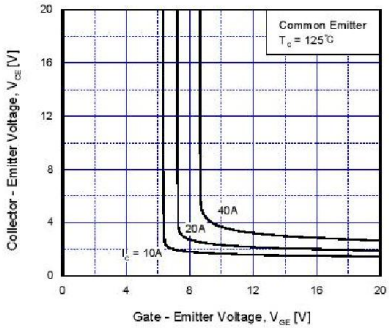

Fig 6. Saturation Voltage vs. V_{GE}

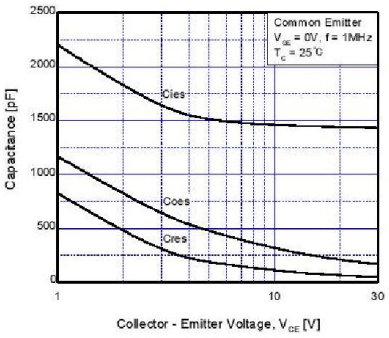

Fig 7. Capacitance Characteristics

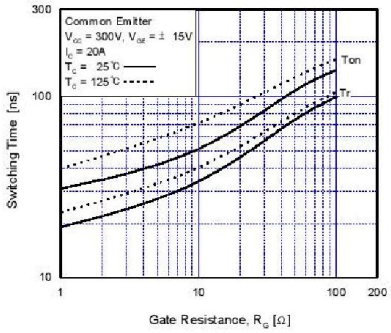

Fig 8. Turn-On Characteristics vs. Gate Resistance

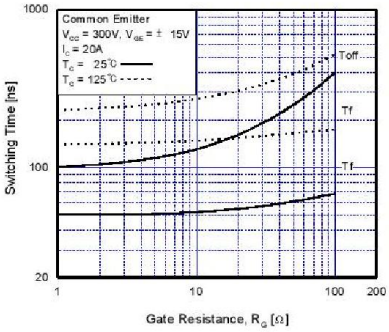

Fig 9. Turn-Off Characteristics vs. Gate Resistance

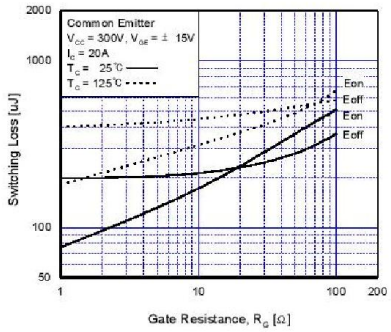

Fig 10. Switching Loss vs. Gate Resistance

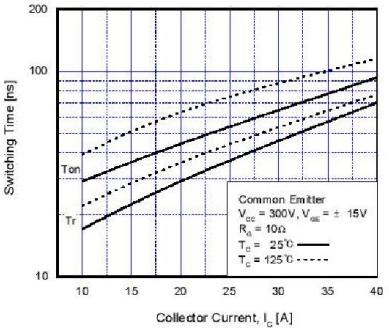

Fig 11. Turn-On Characteristics vs. Collector Current

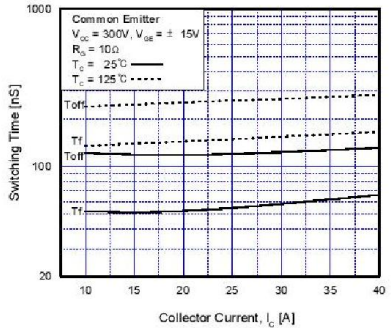

Fig 12. Turn-Off Characteristics vs. Collector Current

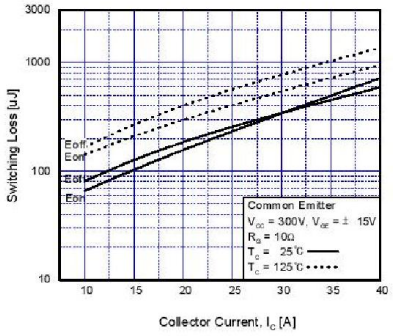

Fig 13. Switching Loss vs. Collector Current

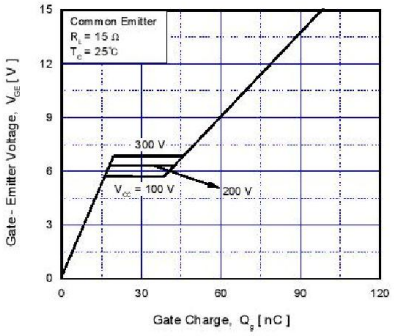

Fig 14. Gate Charge Characteristics

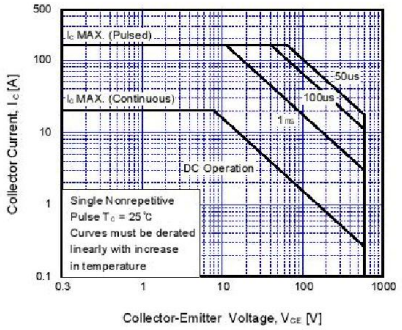

Fig 15. SOA Characteristics

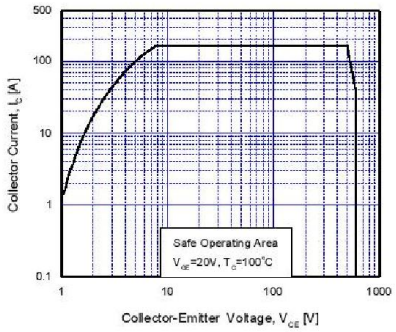

Fig 16. Turn-Off SOA Characteristics

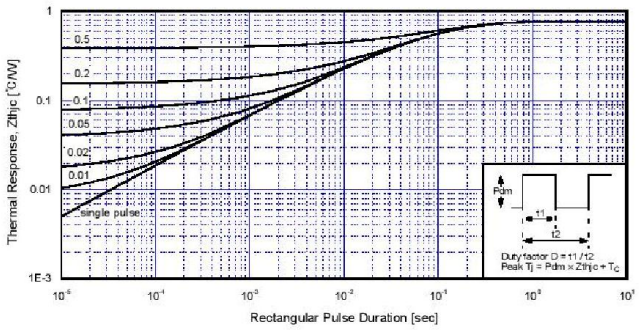

Fig 17. Transient Thermal Impedance of IGBT

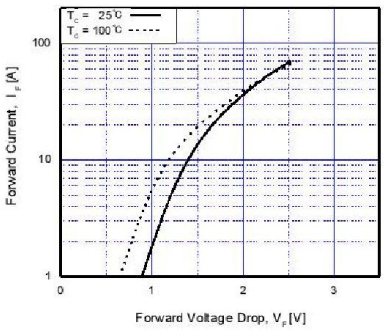

Fig 18. Forward Characteristics

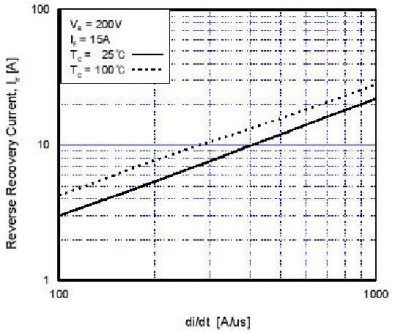

Fig 19. Reverse Recovery Current

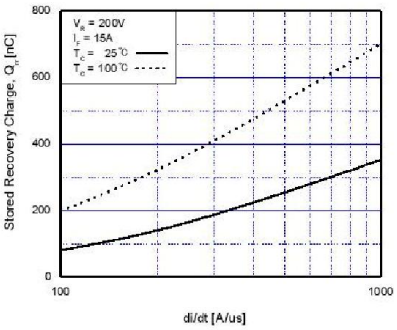

Fig 20. Stored Charge

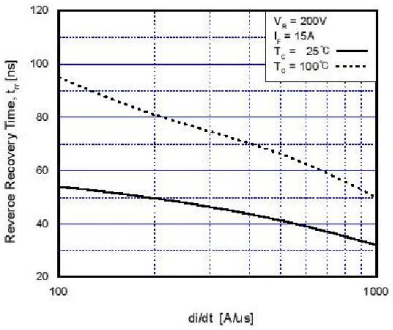

Fig 21. Reverse Recovery Time

Mechanical Dimensions

TO-3PN

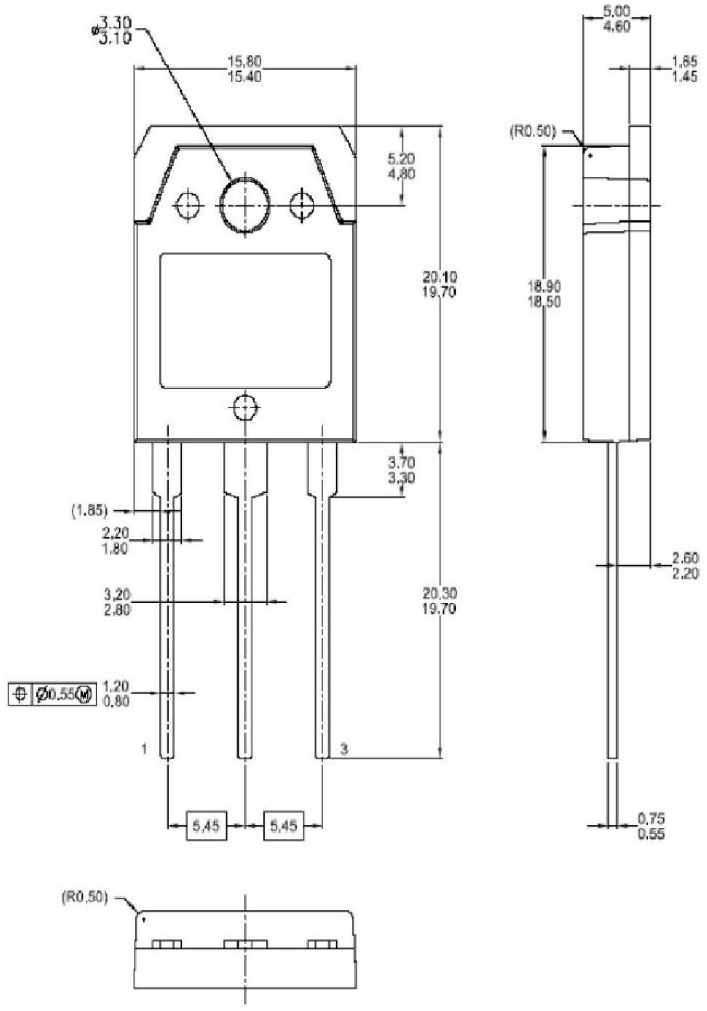

Dimensions in Millimeters

TRADEMARKS

The following are registered and unregistered trademarks Fairchild Semiconductor owns or is authorized to use and is not intended to be an exhaustive list of all such trademarks.

ACEx™	FAST®	MICROWIRE™	SLIENT SWITCHER®	UHC™
Bottomless™	FASTr™	OPTOLOGIC™	SMART START™	UltraFET®
CoolFET™	FRFET™	OPTOPLANAR™	SPM™	VCX™
CROSSVOLT™	GlobalOptoisolator™	PACMAN™	STAR*POWER™	
DenseTrench™	GTO™	POP™	Stealth™	
DOME™	HiSeC™	Power247™	SuperSOT™-3	
EcoSPARK™	I²C™	PowerTrench®	SuperSOT™-6	
E²CMOS™	ISOPLANAR™	QFET™	SuperSOT™-8	
EnSigna™	LittleFET™	QS™	SyncFET™	
FACT™	MicroFET™	QT Optoelectronics™	TinyLogic™	
FACT Quiet Series™	MicroPak™	Quiet Series™	TruTranslation™	

STAR*POWER is used under license

DISCLAIMER

FAIRCHILD SEMICONDUCTOR RESERVES THE RIGHT TO MAKE CHANGES WITHOUT FURTHER NOTICE TO ANY PRODUCTS HEREIN TO IMPROVE RELIABILITY, FUNCTION OR DESIGN. FAIRCHILD DOES NOT ASSUME ANY LIABILITY ARISING OUT OF THE APPLICATION OR USE OF ANY PRODUCT OR CIRCUIT DESCRIBED HEREIN; NEITHER DOES IT CONVEY ANY LICENSE UNDER ITS PATENT RIGHTS, NOR THE RIGHTS OF OTHERS.

LIFE SUPPORT POLICY

FAIRCHILD'S PRODUCTS ARE NOT AUTHORIZED FOR USE AS CRITICAL COMPONENTS IN LIFE SUPPORT DEVICES OR SYSTEMS WITHOUT THE EXPRESS WRITTEN APPROVAL OF FAIRCHILD SEMICONDUCTOR CORPORATION.

As used herein:

1. Life support devices or systems are devices or systems which, (a) are intended for surgical implant into the body, or (b) support or sustain life, or (c) whose failure to perform when properly used in accordance with instructions for use provided in the labeling, can be reasonably expected to result in significant injury to the user.

2. A critical component is any component of a life support device or system whose failure to perform can be reasonably expected to cause the failure of the life support device or system, or to affect its safety or effectiveness.

PRODUCT STATUS DEFINITIONS

Definition of Terms

Datasheet Identification	Product Status	Definition
Advance Information	Formative or In Design	This datasheet contains the design specifications for product development. Specifications may change in any manner without notice.
Preliminary	First Production	This datasheet contains preliminary data, and supplementary data will be published at a later date. Fairchild Semiconductor reserves the right to make changes at any time without notice in order to improve design.
No Identification Needed	Full Production	This datasheet contains final specifications. Fairchild Semiconductor reserves the right to make changes at any time without notice in order to improve design.
Obsolete	Not In Production	This datasheet contains specifications on a product that has been discontinued by Fairchild semiconductor. The datasheet is printed for reference information only.

Rev. H5